THE STUDY OF SPIN GLASS STATE IN DILUTED MAGNETIC MATERIALS AND SEMICONDUCTORS USING MONTE CARLO METHOD AND THEORETICAL ANALYSIS

Habte Dulla Berry

A Thesis Submitted to

The Department of Physics

PRESENTED IN FULFILMENT OF THE
REQUIREMENTS FOR THE DEGREE OF DOCTOR OF PHILOSOPHY (CONDENSED MATTER PHYSICS)

ADDIS ABABA UNIVERSITY
ADDIS ABABA, ETHIOPIA
MARCH 2013

ADDIS ABABA UNIVERSITY
DEPARTMENT OF
PHYSICS

This is to certify that the thesis prepared by **Habte Dulla Berry** Graduate Studies entitled "**The Study of spin glass state in diluted magnetic materials and semiconductors using monte carlo method and theoretical analysis**" in fulfillment of the requirements for the degree of **Doctor of Philosophy (Condensed Matter Physics)** complies with the regulations of the University and meets the accepted standards with respect to originality and quality. .

Dated: March 2013

External Examiner: _____
Prof.Keya Dharamvir

Internal Examiner: _____
Prof. Malnev V.

Research Supervisor: _____
Prof. P. Singh

_____

ADDIS ABABA UNIVERSITY

Date: **March 2013**

Author: **Habte Dulla Berry**

Title: **The Study of spin glass state in diluted magnetic materials and semiconductors using monte carlo method and theoretical analysis**

Department: **Physics**

Degree: **Ph.D.** Convocation: **July** Year: **2013**

Permission is herewith granted to Addis Ababa University to circulate and to have copied for non-commercial purposes, at its discretion, the above title upon the request of individuals or institutions.

Signature of Author

To my family.

Table of Contents

Abstract

Spin glass system is a complex disordered system with a number of local minima separated by entropic barriers. Therefore, Parallel tempering Monte Carlo simulation was used in order to get fast thermalisation (to minimize the relaxation time). Distance dependent interaction coupling in 2D is studied in order to show how a spin glass phase transition occurs when couplings between far away spins are permitted by considering Edwards-Anderson Ising spin glass model. The interaction coupling is a quenched random variable whose probability of being non-zero decays with distance between two spin sites $r_{ij} = |i - j| mod(L/2)$. The interaction coupling is random and its probability distribution is decaying with the distance between the spins ($p(J_{ij}) \propto r^{-\rho}$). The model is studied by changing ρ among three different regimes ($\rho > 2D, 4/3D < \rho < 2D, \rho < 4/3D$) . A phase transition temperature for $\rho = 2, 3, 4$ is obtained.

In the present work, the possibility of existence of spin glass phase using classical Heisenberg model with Edwards-Anderson type of interactions has been explored employing Monte Carlo simulation of Binder parameter (g (L, T)). Previous experimental studies show that there is finite temperature phase transition but this study indicates that there is no finite temperature phase transition in 3D Heisenberg vector spin glass model.

In the dissertation we also explore magnetic properties especially spin glass state, antiferromagnetic state and paramagnetic state of diluted magnetic semiconductors ($A_{1-x}Mn_xA'(A = Zn, Cd$ and $A' = S, Te, Se)$) at critical region using classical Heisenberg spin model with high temperature series expansion extrapolated with

padé approximants. The critical exponents associated with magnetic susceptibility ($\gamma \simeq 1.38 \pm 0.1$) and correlation function ($\nu \simeq 0.8 \pm o.1$) were also obtained.

Acknowledgements

First of all I would like to thank the almighty God.

I am thankful to school of graduate studies of Addis Ababa University for financial support in my all research activities.

I am deeply indebted to my advisor, Prof. P. Singh, not only academically but also in every aspect of my life after I met him. I am thankful to him for giving me opportunities to indulge myself in this wonderfully intriguing research field, guiding me to the right research direction, and sharing his deep insights in to physics.

I would like to thank the department of Physics for facilitating all the necessary materials while I am doing my research work. I am thankful to Dr. Belayneh Mesfin(head department of Physics), Dr. Lemi Demeyu , Dr. Mulgeta Bekele, Dr. Feseha Kasahun for their valuable suggestion. I would also like to acknowledge my sponsor, Dilla University, for the financial and material support through out my study. Last but not least I would like to express my thanks to all my family members especially to my wife Belaynesh Habtemariam and my daughter Blen Habte for their endless support and love.

List of Figures

List of Tables

General Introduction

The biggest challenge in recent days in statistical physics is the study of random system. Therefore systems with quenched disorder like spin glasses have attracted much attention during the past three decades. In order to study such systems people use different computational techniques. One of these techniques is the Monte Carlo method which is a powerful class of algorithms that is not only used in physics but also in other fields like Engineering, Chemistry, Biology, Material science, Finance and Statistics. In some fields such as in condensed matter physics, many problems are characterized by conflicting forces on a microscopic level, for bidding simultaneous minimization. This effect is commonly known as frustration and usually makes systems very hard to simulate using traditional Monte Carlo methods. Recently, many numerical methods have been developed in order to improve the efficiency of Monte Carlo simulations in systems with slow dynamics like spin glasses even if the problem has not been solved completely. Nowadays the standard method to study such systems at equilibrium is parallel tempering, also known as replica exchange Monte Carlo [1, 2]. Monte Carlo simulation techniques like parallel tempering are often used to evaluate low temperature properties and find ground states of disordered systems. Systems like spin glasses at low temperature have a lot of local energy minima in the phase space and these minima are separated by free energy barriers[3, 4, 5, 6]. If we

want to properly thermalize the system, all the phase space has to be visited. But in this case the time needed by the system to escape from local minima increases with lowering the temperature . One possible way to avoid such a problem is simulating the system by using parallel tempering method. To each of replica we attribute a different temperature , in such away to span a range including high and low temperature values. In this dissertation we use parallel tempering Monte Carlo simulation, in order to study the spin glass transition in 2D Ising spin glass with power low decaying interactions. In addition to that, we use ordinary Monte Carlo simulation to identify spin glass state at 3D vector (Heisnberg) spin model. Finally, we give theoretical analysis for the magnetic properties (magnetic susceptibility, correlation function and magnetic specific heat) of diluted magnetic semiconductors at critical region by taking in to consideration of high temperature series expansion approach followed by Padé approximants.

This dissertation is organized as : (I)Literature Review;(II)Parallel tempering Monte Carlo simulation of 2D Ising spin glass with distance dependent interactions ; (III) Monte Carlo simulation of spin glasses using vector spin (Heisenberg) model in 3D; (IV) spin glass state in II-VI diluted magnetic semiconductors at the critical region using high temperature series expansion extrapolated with Padé approximants; (V) Summery; and Future plan.

Chapter 1

Literature Review

In this chapter we will give brief explanation about the materials and the methodology that we use in this dissertation. In section(1.1) a brief discussion about semi magnetic semiconductors and their advantages; in section(1.2) about Ising model and its exact solution according to L. Onsager and in section (1.3) we will see about the methodology that we use i.e. about the algorithms of Monte Carlo simulation and exchange Monte Carlo simulation.

1.1 Diluted Magnetic Semiconductors

During the last few decades, the electronics industry has made a big progress , with its basic unit, the integrated circuit(IC) chip bringing down to a large number of day to day applications. This is because of the scientific community tried to conduct researches in this regard. The transistor is the smallest electronic component of such IC chip , which was fabricated in the late 1940s by scientists at Bell labs. Through time, the metal oxide semiconductor field effect transistor (MOSFET) invented as the most widely used transistor structure. In 1965 Gordon Moore, then at Fair

child Semiconductor, proposed what has now come to be known as Moore's law [7]. The most important idea of the law was that the number of transistors built on a wafer would double every two years, and that this scaling would be the key improving performance and profitability in the micro electronic industry. However, during scaling some problems appear such as the need for very thin gate oxide layers , that could be leaky and need constant refreshing. This would lead to unacceptably high power consumption, which could act as an impediment to further scaling down. Thus, these new approaches have constantly been investigated in order to further the miniaturization of micro electronics technology. One of such possibility is to incorporate the role the spin of the charge carriers in addition to their charge in devices. Semiconductors doped with magnetic impurities are being studied in a great hope to develop spintronics the new kind of electronics that needs to be fully exploited, in addition to the charge degree of freedom as in the usual electronics, also the spin of the carriers[8].There are two very important advantages of doing this, the first being the ability of magnetic materials to remember their spin state, without any refresh. This could allow us to integrate logic and storage processes and potentially lead to instant-on computers , where no boot up is required. The other advantage is that relatively low energy is required to manipulate the orientation of spin of a carrier, which could allow development of low power spintronic devices.

There are several classes of semiconducting materials that are characterized by the random replacement of a fraction of the original atoms by magnetic atoms. The materials are usually known as diluted magnetic semiconductors (DMS) or semi-magnetic semiconductors (SMSC).The first so-called diluted magnetic semiconductors (DMS) were II-VI semiconductor alloys like $Zn_{1-x}Mn_xTe$ and $Cd_{1-x}Mn_xTe$ [9] originally

studied in the 1980s. These materials are either spin glasses or have very low ferromagnetic (FM) critical temperatures T_c ($\sim few K$) [10] and are, therefore, inadequate for technological applications which would require FM order at room temperature. At the beginning, the study of II-VI DMSs has attracted the interest of researchers since their discovery because of the following important properties.

• Unique electronic properties: Because of the wide variety of both the semiconducting host materials and magnetic atoms provide materials which range from wide gap to zero gap semiconductors, and lead to many different types of magnetic interaction. The properties of these materials may depend on the concentration of the magnetic impurities. For instance, the band gap E_g , of $Hg_{1-x}Mn_xTe$ can even change from negative to positive and such property becomes favorable as far as designing infrared devices is concerned. The dependence of E_g of $Hg_{1-x}Mn_xTe$ on x is given in Fig. 1.1[11].

• Broad phase behavior: With basic ingredients such as different Mn concentration x and temperature T, each II-VI DMS presents a different (phase) property, but their concentration (x)-T magnetic phase diagrams are very similar. As shown below in Fig. 1.2 is the magnetic phase diagram of $Cd_{1-x}Mn_xTe$ obtained from specific heat and magnetic susceptibility measurements [13, 12]. The DMS materials can be considered as consisting of two interacting subsystems. The 1^{st} one of these subsystem is the system of delocalized conduction and valence band electrons/holes. The 2^{nd} one is the random,and diluted system of localized magnetic moments associated with the magnetic atoms. These two subsystems interact with each other by the spin exchange interaction. It is known that both the structure and the electronic properties of the semiconducting host crystals are very helpful for the study of the basic mechanisms

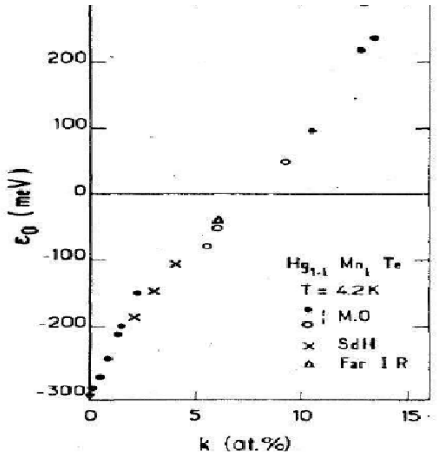

Figure 1.1: *Schematic representation of the band gap dependence of* $Hg_{1-k}Mn_kTe$ *on Mn concentration* k *[11].*

of the magnetic interactions coupling the spins of the band carriers and the localized spins of magnetic ions. The coupling between the localized moments results in the existence of different magnetic phases such as paramagnetism, spin glasses and antiferromagnetism.

• Important magnetic phenomena: As explained above, if there is no spin exchange integral between the band electrons and localized magnetic moments, DMS materials are just the same as the ordinary semiconductors. But if there is the spin exchange interaction, however, DMS materials present many important properties, such as very big Lande g -factors, extremely large Zeeman splitting of the electronic bands, giant Faraday rotation, and huge negative magnetoresistance. Therefore, to study the properties of DMS, one has to first understand the spin exchange interaction between

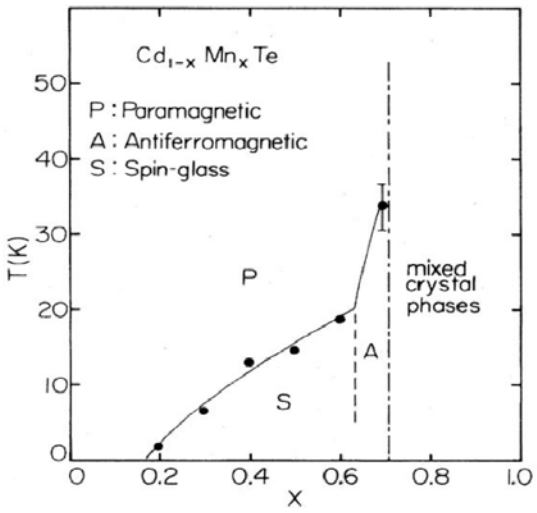

Figure 1.2: *Schematic representation of magnetic phase diagram of* $Cd_{1-x}Mn_xTe$. *P, A, and S stand for paramagnet, antiferromagnet and spin glass respectively* [*12*].

the localized magnetic ions and band electrons.

Since the first discovery of DMS in II-VI semiconductor compounds [13], more than two decades have passed. The present discovery of ferromagnetic DMS based on III-V semiconductors $In_{1-x}Mn_xAs$ and $Ga_{1-x}Mn_xAs$[14] has led to a surge of interest in DMS for possible spintronics applications and this is because of relatively higher temperature of the alloys Mn doped III-V semiconductors $In_{1-x}Mn_xAs$ [15, 16] and $Ga_{1-x}Mn_xAs$ [18, 19], due to the development of molecular beam epitaxy (MBE)-growth techniques. The current high T_c record of 173K achieved in Mn-doped GaAs by using low temperature annealing techniques [20, 21, 22] is promising, but still too low for actual applications. Studies showed that ferromagnetic phase in this material exists because of the following facts:-

1.Ruderman, Kittel, Kasuya and Yosida (RKKY)interaction

Indirect exchange interaction coupling between magnetic moments are relatively at large distances. This coupling mechanism is the dominant exchange coupling in metals where there is little or no direct overlap between neighboring magnetic impurities. The case of this interaction coupling is believed to be an intermediary which in metals are the conduction electrons (itinerant electrons) or holes. This type of exchange couplig was first explained by Ruderman and Kittel [23] and later extended by Kasuya [24] and Yosida [25] to give the theory now generally known as the RKKY interaction. Ohno et al. explained the ferromagnetism in $Ga_{1-x}Mn_xAs$ for Mn concentration x = 0.013 using the RKKY mechanism [16]. In the interaction Hamiltonian,

$$H = -J_{ij}^{RKKY} S_i.S_j, \tag{1.1.1}$$

the interaction coupling coefficient J_{ij}^{RKKY} is assumed [17],

$$J_{ij}^{RKKY}(r) = J_0 r^{-4} exp(-\frac{r}{l})[sin(2K_F r) - 2K_F r cos(2K_F r)], \tag{1.1.2}$$

where the Fermi wave number $K_F = \sqrt[3]{\frac{1}{3}\pi^2 n_c}$ and K_F is the radius of the conduction electron/hole Fermi surface, r is the distance away from the origin where a local moment is placed. The RKKY exchange integral coefficient, J , oscillates from positive to negative as the distance between of the ions changes with the period determined by the Fermi wave vector K_F^{-1} and has the damped oscillatory nature shown in Fig. 1.3. Therefore, based up on the distance between a pair of ions, their magnetic interaction coupling can be ferromagnetic or antiferromagnetic. A magnetic impurity induces a spin polarization in the conduction electrons in its nearest neighbor. This spin magnetic moment in the itinerant electrons is felt by the moments of other magnetic impurity within range, leading to an indirect coupling.

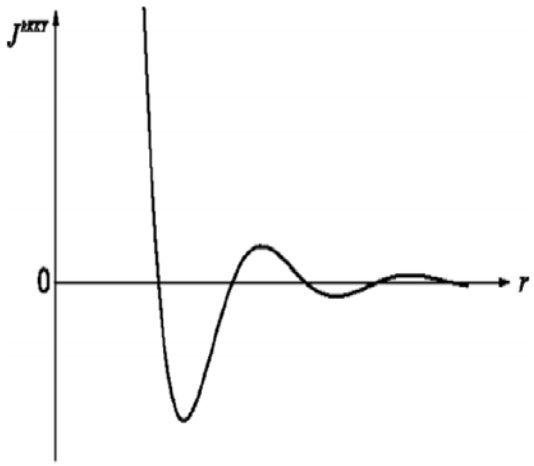

Figure 1.3: *Schematic representation of Variation of the RKKY coupling constant, J , of a free electron gas in the neighborhood of a point magnetic moment at the origin $r = 0$ [16].*

2. Zeners model: This model is a continuous-medium limit of the RKKY model. The model was for the first time investigated by C. Zener in 1950 [26] to explain the parallel(ferromagnetic)spin coupling in transition metals. In the same way to the RKKY model, it represents an exchange interaction between charge carriers and localized spins. The Hamiltonian of Zeners model in a transition metal is [26]

$$H_s = \frac{1}{2}\alpha S_d^2 - \beta S_d S_c + \frac{1}{2}\gamma S_c^2, \tag{1.1.3}$$

where S_d and S_c are the mean magnetization of the d-shell electron and the conduction electron respectively, and α, β, and γ are the three coupling constants.

Much work has been produced investigating their electronic , magnetic, optical, thermal, statistical and transport properties , in many journals, and even in many

prestigious magazines [27]. This interest not only comes from the DMS themselves as good theoretical and experimental subjects , but also can be better understood from a broader view from the relation of DMS research with spintronics [28]. Spintronics (spin + electronics) means the study of the role played by electron (and nuclear) spin in solid state physics, and materials (devices) that specifically include spin properties in addition to or apart from the charge degrees of freedom. Spin relaxation and spin transport in metals and semiconductors are of important research area not only for being basic solid state physics issues, but also for the already demonstrated potential these phenomena have in the present technological advancement. There is a famous Moore's Law in the conventional electronics industry, that it says the number of transistors that fit on a computer chip will double every 18 months. Moore's Law may soon face some fundamental problems . Different researchers think that there will eventually be a limit to how many transistors they can cram on a chip. But even if Moore's Law could continue to diminish the size of the chips, small electronic devices are plagued by a big obstacle : energy loss, or dissipation, as signals pass from one transistor to the next. Lining up all the tiny wires that connect the transistors in a Pentium chip, and the total length would stretch almost in miles. A huge amount of useful energy can be wasted as heat as electrons travel that distance. Spintronics, that considers spin as the information carriers, unlike with conventional electronics, consumes very less energy and these devices are capable of higher speed. The most widely studied DMS in the early 1990s were II -VI compounds (like CdTe , ZnSe , CdSe , CdS, etc.), with the replacement of transition metal ions at the cation site (e.g., Mn, Fe or Co). Other promising materials based on IV- VI (e.g., PbS, SnTe) and most importantly, III-V (e.g., GaAs, InSb) crystals are under investigation. Most

commonly, Mn ions are used as magnetic dopants.

1.1.1 Advantages of Studying DMSs

Its obvious that, the possibility of using the spin and the charge of the electrons for information processing will have numerous application in recent technology and it is the basic theme of spintronics as mentioned above. The spintronics devices (for instance the transistor of Datta and Das[29]) to work, polarized carriers have to be injected into a semiconductor, for example using ferromagnetic contacts . However, these devices have not been fabricated yet. Because of the conductance mismatch between metals and semiconductors it is very difficult to inject net spin polarization in these materials[30].

1.2 The Ising Model

The model was first suggested to Ising by his PhD thesis supervisor, Lenz. Then, Ising solved the one dimensional model, and on the basis of the fact that the one dimensional model had no phase transition, he concluded that there was no phase transition in any dimension. But in 1944 the 2D Ising model(with no applied magnetic field) was solved by L.Onsager. Nowadays, the model is widely studied and is the best understood model of the whole field of statistical physics. The Ising model is a model of ferromagnetism. It consists of a number of spins s_i that point either up ($s_i = +1$)or down ($s_i = -1$) and are arranged on a regular lattice of dimension D. Each of the spins only interacts with its 2D direct neighbors and the energy of the

system is given by the Hamiltonian

$$E = -\sum_{\langle ij \rangle} s_i s_j. \tag{1.2.1}$$

Where the sum over $\langle ij \rangle$ denotes a sum over all neighboring pairs of spins. In this thesis we used the above Hamiltonian and the following algorithm in order to check if the Monte Carlo trial move is acceptable or not. That is, the spins then either flip or not by calculating the energy difference between the considered spin and its 4 nearest neighbors using the formula:

$$\Delta E = -2J s_{ij}(s_{ijl} + s_{ijr} + s_{iju} + s_{ijd}), \tag{1.2.2}$$

where j_l, j_r, j_u, j_d left, right,up, and down neighbor spins respectively. The spin then directly flips if$\Delta E \leq 0$. But if $\Delta E > 0$, we have to generate a random number in between 0 and 1. Then just by using Boltzmann factor $exp(-\frac{\Delta E}{k_B T})$ we can decide whether the spin is flipped or not. That means if that random number is less than that of the probability distribution , then there is a spin flip, otherwise not. As we mentioned at the beginning of this section, the model was thought not to exhibit phase transitions in any dimension, but immediately the situation turned out that it shows a broken symmetry phase for two or more dimensions[31]. In addition to its simplicity it is therefore an interesting model for understanding the behavior in the vicinity of critical points. The phase transition is between a high temperature phase where all spins are pointing more or less in random directions and an ordered low temperature phase where almost all spins of the lattice have the same alignment. When looking at the equation above we can see that the model is symmetric to flipping all the spins at the same time ($s_i^{'} = -s_i$). In the ordered phase the system can therefore be either in a state where almost all spins are +1 or where almost all of them are -1.

1.2.1 Exact solution of the two-dimensional (2D) Ising model on finite squared lattices

Even if there are exact solutions of both the one-dimensional Ising model and the two-dimensional Ising model in zero external magnetic field, but 2D case is the more interesting of the two since it exhibits a second order phase transition. However for more than 2D cases, exact solutions of the Ising model are still unknown. While these solutions for the two-dimensional Ising model in zero external magnetic field,at first proposed by L.Onsager, is valid only in the thermodynamic limit, exact calculations on finite squared lattices are given by A. E. Ferdinand and M. E. Fisher[32]. According to their studies, exact expressions of the internal energy per spin($\frac{E_{mn}}{mn}$) and the specific heat per spin($\frac{(c_V)_{mn}}{k_B mn}$) can be defined by evaluating the canonical partition function

$$Z_{mn} = \frac{1}{2}(2sinh(2K))^{\frac{1}{2}mn}\sum_{i=1}^{4} Z_i(K), K = \frac{1}{K_B T}, \tag{1.2.3}$$

for an (mn) squared lattice with periodic boundary conditions and coupling constants $J_x = J = J_y$ in zero external magnetic field. The partial partition functions Z_i are defined as follows:

$$\begin{aligned} Z_1 &= \prod_{r=0}^{n-1} 2cosh(\tfrac{1}{2}m\gamma_{2r+1}), \\ Z_2 &= \prod_{r=0}^{n-1} 2sinh(\tfrac{1}{2}m\gamma_{2r+1}), \\ Z_3 &= \prod_{r=0}^{n-1} 2cosh(\tfrac{1}{2}m\gamma_{2r}), \\ Z_4 &= \prod_{r=0}^{n-1} 2sinh(\tfrac{1}{2}m\gamma_{2r}). \end{aligned} \tag{1.2.4}$$

The internal energy per spin is then given by

$$\frac{E_{mn}}{mn} = -\frac{J}{mn}\frac{dlnZ_{mn}}{dK} = -Jcoth(2K) - \frac{J}{mn}[\sum_{i=1}^{4} Z_1'][\sum_{i=1}^{4} Z_1]^{-1}, \tag{1.2.5}$$

while the specific heat per spin is

$$\frac{(c_V)_{mn}}{k_B mn} = \frac{K^2}{mn}\frac{d^2 lnZ_{mn}}{dK^2} = -2K^2 csch^2(2K) + \frac{K^2}{mn}[\frac{\sum_{i=1}^{4} Z_1''}{\sum_{i=1}^{4} Z_1'} - (\frac{\sum_{i=1}^{4} Z_1'}{\sum_{i=1}^{4} Z_1})^2], \tag{1.2.6}$$

where the primes denote differentiation with respect to K. Equations(1.2.5)and(1.2.6)enable us to compare Monte Carlo estimates of the internal energy and the specific heat from simulating the Ising model on finite squared lattices against exact calculations.

1.3 Monte Carlo Methods

Monte Carlo simulation is one of a computer simulation techniques that has been broadly applied to discover properties of physical system. The main advantage of such a technique is that it leads us to change physical parameters at will. Monte Carlo methods are the computational techniques which solve a problem by generating suitable random numbers and observing that fraction of the numbers obeying some properties. The technique is useful for obtaining numerical solutions to problems which are too complicated to solve analytically. It was named the Monte Carlo method by S. Ulam after the Monte Carlo casino based on random number generation. Monte Carlo methods are based on the idea of repeated random sampling of the search space and the application of statistics to compute the searched value. The method tend to be used when it is unfeasible or impossible to compute an exact result with a deterministic algorithm. Monte Carlo algorithms are usually defined as a class of algorithms that use random sampling to solve a problem. Although the first Monte Carlo algorithm dates back to the middle of the nineteenth century, they only gained their modern name and wide spread acceptance with the advent of electric computers [33]. These days, Monte Carlo techniques are used in wide variety of fields including Chemistry, Biology, Material Science, Finance, Statistics and, of course, Physics. In general, as we mentioned above Monte Carlo simulation is a stochastic method to compute any quantity of a system that has several degrees of freedom. For instance

we can consider Ising ferromagnetic system with lattice size N and each lattice site is occupied by a spin. The total number of spin configurations in the system is 2^N and the thermal average of any physical quantity Y, that can be magnetization, specific heat etc .. can be defined as

$$\langle Y \rangle_T = \sum_{i=1}^{2^N} y_i p_i, \tag{1.3.1}$$

where y_i is its value at state i and p_i is the Gibbs probability at this state. The probability p_i, can be given by

$$p_i = \frac{exp(-\beta E_i)}{Z}; Z = \sum_i exp(-\beta E_i), \tag{1.3.2}$$

where E_i is the energy of state i and Z is the partition function. Therefore, to calculate this even for small lattice size takes huge computer memory and uses enormous amount of computer time. In order to avoid such a complication, one can sample the microstates randomly. But as the system could spend most of its time in the corresponding microstates of the equilibrium state, so that the calculation of thermal average using this random sampling method would give unreliable result as the method might pick up states that are of less importance. To avoid this problem one can use importance sampling technique which was firstly introduced by Metropolis. The general idea of every Monte Carlo algorithm is to solve an integral by sampling random points of the integral. To understand how a Monte Carlo algorithm works, it is useful to remember that almost every problem in statistical mechanics can be expressed as calculating the expectation value of a quantity B for a certain ensemble.This value can be expressed as a sum (or for the continuous case an integral) of the form:

$$\langle B \rangle = \sum_{s \epsilon \Omega} B(s) P(s) = \sum_{s \epsilon \Omega} B(s) \frac{w(s)}{Z}, \tag{1.3.3}$$

where Ω is the set of all possible states (also called configurations) of the system, w(s) is the relative probability that the system is in this particular states and $Z = \sum_{s\epsilon\Omega} w(s)$ is the normalization constant for the probabilities.

1.3.1 The Metropolis Algorithm

If we have an observable B, then we can determine the expectation value of the observable as

$$\langle B \rangle = \frac{\sum_r B_r \exp(-\beta E_r)}{\sum_r \exp(-\beta E_r)}, \tag{1.3.4}$$

in this case B_r is the value of B for the state r. We have a system that has a discrete number of states[34] and by using a machine we can calculate the observable B for each state and weigh these values by their Boltzmann factors to find the average. This might be possible for a system with a small number of states, but if we have large spin lattices, it is not possible to get a solution in this way. Therefore , we have to use the Monte Carlo approach for such a case. Instead of sampling a lot of states and then weighing them by their Boltzmann factors, it makes sense to choose states based on their Boltzmann factors and then to weigh them equally. This is known as the metropolis algorithm, which is an importance sampling technique. The algorithm is described as :

(1) a trial configuration is made by flipping one spin.

(2) Calculate the energy difference of the trial state relative to the present state i.e. $\Delta E = E_{new} - E_{old}$. Where E_{new} is the energy after the trial move and E_{old} is the energy before trial move.

(3) If the energy difference is less than or equal to zero, then the trial state is energetically favorable and thus accepted. Otherwise , a random number[35, 36]

between zero and one should be generated and the trial move is only accepted if the probability distribution is greater than the random number generated. Let us now define the transition probability as $T(o \rightarrow n)$ to go from configuration old to new. We denote the number of points in any configuration old by k(o) and new by k(n). In equilibrium, the average number of trial moves that result in the system leaving state old (o) must be exactly equal to the number of accepted trial moves from all other states new(n) to state old(o). In other words, in equilibrium the average number of accepted moves from old state(o) to any other new state(n) is exactly canceled by the number of reverse moves. This implies that the following condition:

$$k(o)T(o \rightarrow n) = k(n)T(n \rightarrow o), \tag{1.3.5}$$

is called the detailed balance. Now, we denote the transition matrix[37] that determines the probability of proposing a trial move from old to new configuration by $q(o \rightarrow n)$. Our next step is to check whether the trial move is accepted or rejected. In order to check this situation let us assume that the probability of accepting a trial move from old state to new state by $a(o \rightarrow n)$. Therefore, we can define the transition probability in terms of transition matrix and acceptance probability, i.e.,

$$T(o \rightarrow n) = q(o \rightarrow n)a(o \rightarrow n). \tag{1.3.6}$$

The first Monte Carlo algorithm applied to physics was a Marcov chain Monte Carlo algorithms called the Metropolis algorithm[38]. As its formulation is quite general, many of the Monte Carlo algorithms used today can be seen as special cases of the Metropolis algorithm. If the transition probability is symmetric , we can write the following expression.

$$k(o)a(o \rightarrow n) = k(n)a(n \rightarrow o). \tag{1.3.7}$$

Then we have the following probability

$$\frac{a(o \to n)}{a(n \to o)} = \frac{k(n)}{k(o)} = \exp[-\beta[u(n) - u(o)]], \tag{1.3.8}$$

but this probability cannot exceed one. Where u(n) is energy of the new state and u(0) is the energy of the old state. Therefore we can use the following probability just to decide whether a trial move is to be accepted or rejected:

$$a(o \to n) = \exp[-\beta[u(n) - u(o)]]. \tag{1.3.9}$$

If$\Delta u \leq 0$

$$a(o \to n) = 1. \tag{1.3.10}$$

If$\Delta u > 0$ then by generating a random number between zero and one we can decide the trial move is accepted or not.

1.3.2 Parallel Tempering

The method of parallel tempering[39, 40, 41] is a Monte Carlo scheme[42, 43] that has been derived to achieve good sampling of systems that have a free energy landscape with many local minima. Just to implement a parallel tempering algorithm[44] one needs to make M replicas[45] of the system(ensemble) to be analyzed, each of which characterized by different temperatures[46] $T_1 > T_2 ... > T_M$. The main idea of this method is to simulate independently the standard Monte Carlo for each copy, all of them at different temperatures and to swap periodically the configurations of two randomly chosen temperatures[47]. The purpose of this swap is to avoid that replicas at low temperatures get stuck in local minima. Thus the highest temperature,T_1 , is set in the high-temperature phase, where relaxation time is expected to be very

short and there exists only one minimum in the free energy space. Systems with sufficiently high temperature pass all the energy barriers in the system. The low temperature systems , on the other hand, mainly probe the local energy minima. For a given replica, the swap moves induce a random walk in temperature space. This random walk allows the replica to overcome free energy barriers by wandering to high temperatures where equilibration is rapid and return to low temperatures where relaxation time can be long. By doing so, we can overcome the energy barrier and increase the speed of relaxation to equilibrium in the the simulation if the temperature difference is not too large. After a fixed number of Monte carlo sweeps, a sequence of swap moves, (the exchange of two replicas at neighboring temperatures , T_i and T_{i+1}) is suggested and accepted or rejected according to the metropolis algorithm, i.e. with probability one for $\Delta\beta\Delta E \leq 0$ and with probability $\exp(-\Delta\beta\Delta E)$ for $\Delta\beta\Delta E > 0$ which implies that:- The probability of exchanging two copies depends on the intersection of energy distributions at the two temperatures. The parallel tempering algorithms , indeed, guarantee that an exchange is proposed between two configurations that can be in equilibrium configurations both T_i and T_{i+1}). This condition is implemented in the algorithm

$$P(\sigma_i, E_i, T_i \rightarrow \sigma_{i+1}, E_{i+1}, T_{i+1}) = Min[1, \exp(-\Delta\beta\Delta E)], \tag{1.3.11}$$

where $\Delta\beta = (\frac{1}{T_{i+1}} - \frac{1}{T_i})$ is the difference between the inverse temperatures by assuming that $k_B = 1$ and $\Delta E = E_{i+1} - E_i$ is the difference in energy of the two replicas.

Chapter 2

Theory of Spin Glasses

In this chapter we will concentrate on Monte Carlo simulation of 2D Ising spin glass model. However, according to previous studies there is no spin glass phase for 2D Ising spin model for the nearest neighbor interactions. Therefore,in order to show spin glass state we will use power law decaying interactions.

2.1 Introduction

Canella and Mydosh discovered the Spin Glass phenomenon in 1972[48] while performing standard systematic experimental measurements on dilute alloys of magnetic elements in non-magnetic metal hosts. They made the remarkable and entirely unexpected discovery that is characterized by a sharp cusp in the variation with temperature of the low field linear ac susceptibility $\chi(T)$ of dilute AuFe alloys[48]. The presence of this cusp shows that there is a hidden but well defined phase transition in this dilute alloy, although the magnetic moments are distributed at random and interactions between spins are complex. Careful experimental work on a number of dilute magnetic alloys have shown that the nonlinear susceptibility (with terms proportional to H^3, H^5 etc.) diverges at the cusp temperature T_c, and that critical exponents can

be defined and measured, confirming the existence of a bona fide phase transition of an entirely new type. Numerous materials have now been shown to be spin glasses, and their properties have been studied extensively. Unusual dynamic and memory effects have attracted particular attention.

In 1975 the theoretical spin model was introduced by Edwards and Anderson (EA)[49];in which magnetic moments are placed on all sites of a regular spin lattice but the magnetic interactions between the nearest neighbor spins are chosen to be random, with their signs are arbitrarily distributed. The EA spin glass order parameter is defined as $q_{SG} = lim_{t\to\infty} < s_i(0)s_i(t) >$. Model spin glasses, mainly of the EA family, have been the subject of thousands of theoretical and numerical studies. During the last decades a lot of research has been conducted to get a clear insight about spin glasses . This effort was interesting to better understand the spin glass phenomena and other related complex systems in different fields. Spin glasses are materials whose ground state at low temperature is a frozen disordered state instead of an ordered one, as it is the case for ferromagnets , or a periodic one, as it is the case for antiferromagnets. No long-range order is present in spin glasses. All these features are the consequence of frustration. In this context frustration can be defined as the conflict among different interactions which means not all of the interactions can be mutually satisfied.

In spin glasses, frustration is believed to be a consequence of quenched disorder(the randomness in the interactions)which means that the interactions between spins and /or their locations have constrained disorder. Due to this disorder in the interactions, the spin glass phase is an example of spontaneous cooperative freezing

of the random spin orientations[52, 51, 50]. Spin glasses are realized typically in alloys of a magnetic metal and a non magnetic metal, because the Ruderman- Kittel-Kasuya-Yosida (RKKY) exchange interaction between the magnetic moments alternate in sign as a function of the distance and some of the magnetic moment pairs interact ferromagnetically so that some antiferromagnetically[53]. In particular, when the interactions are ferromagnetic for some bonds and antiferromagnetic for others, then the spin orientation cannot be uniform in space, unlike the ferromagnetic system, even at low temperatures. Under such a circumstance it sometimes happens that spins become randomly frozen in time. This is the intuitive picture of the spin glass phase.

2.2 Phase transitions and critical exponents

Conventionally, we can categorize the phase transitions into those of first-order and those of higher than first-order (second-order), also called continuous phase transitions[54, 55]. The 1^{st} order phase transitions involve a latent heat, which means the system absorbs or releases a fixed amount of energy. According to the Ehrenfest classification of phase transitions, this causes a discontinuity in the first derivative of the Gibbs free energy with respect to a thermodynamic variable. Continuous phase transitions involve no latent heat, but there is a discontinuity in higher than first-order derivatives of the Gibbs free energy. Therefore, this leads to divergent susceptibilities which in turn are related to effective long-range interactions between the systems constituents. To understand the strength of these interactions, we introduce the so called two-point spin correlation function $\gamma(i,j) = \langle S_i \cdot S_j \rangle$. Considering that the lattice is isotropic, which should be valid for macroscopic systems, γ relays only on

the distance $r = |i-j|$. Since the existence of an external field makes γ being different from zero even if the spins S_i and S_j do not interact, a more suitable measure for correlations due to spin-spin interactions is the connected two-point spin correlation function

$$\gamma(r) = \langle S_i \cdot S_j \rangle - \langle S_i \rangle \langle S_j \rangle. \tag{2.2.1}$$

The asymptotic form of $\gamma(r)$ for large r, compared with intermolecular distances, is given by a power law

$$\gamma(r) \propto \frac{1}{r^{d-2+\eta}}, \tag{2.2.2}$$

r large and $T = T_c$, where η is a critical exponent, and d is the spatial dimensionality. For $T \neq T_c$, $\gamma(r)$ cannot be represented by a power law. In fact, for small values of the reduced temperature $t = \frac{(T-T_c)}{T_c}$ it behaves as

$$\gamma(r) \propto e^{\frac{-r}{\xi}}, \tag{2.2.3}$$

r large and $0 < |t| \ll 1$, with ξ being the correlation length. For $T \neq T_c$, fluctuations of the system's quantities are of all sizes up to ξ , but fluctuations that are significantly larger are exceedingly rare. As $T \to T_c$, ξ grows without limits. One finds that

$$\xi \propto |t|^{-\nu}, \tag{2.2.4}$$

$T \to T_c$ and $h = 0$, where ν is a further critical exponent. Actually, there are more than two of these critical exponents, each defined by a power law, describing the behavior of the critical system:

specific heat: $c_v \propto |t^{-\alpha}|$, $T \to T_c$, h=0,

magnetic susceptibility: $\chi \propto |t^{-\gamma}|$, $T \to T_c$, h=0,

correlation function: $\gamma(r) \propto \frac{1}{r^{d-2+\eta}}$, $T = T_c$, h=0.

Knowing critical exponents of a simple-to-study system, it is their universality that allows to give predictions to the behavior of systems of the same universality class systems of the same dimensionality and with the same critical exponents without being familiar with their exact microscopic details.

2.3 The Models

Arrangement of atoms in a crystal is periodic but the situation in spin glass is quite different. Here in glasses the random locations of atoms never change into another set of random locations. A state with spatial randomness apparently does not change with time. The term spin glass implies that the spin orientation has a similarity to this type of location of atom in glasses : spins are randomly frozen in spin glasses. The goal of the theory of spin glasses is to clarify the conditions for the existence of spin glass states. Nowadays , the study of spin glasses is an active and controversial area of statistical physics. It is established within mean-field theory[57, 58] that the spin glass phase exists at low temperatures when random interactions of certain types exist between spins. Here we consider the Edwards-Anderson spin glass model[59], which consists of a set of N Ising spins $s_i = \pm 1$. Its Hamiltonian is

$$H = -\sum_{\langle ij \rangle} J_{ij} s_i s_j. \tag{2.3.1}$$

Where ($\langle ij \rangle$) indicates a sum over nearest neighbors. The coupling constants or bonds , $J_{ij}s$ are independent random variables drawn from a given distribution with mean zero and variance one. Here the spin variables are considered to be of the Ising type($s_i = \pm 1$) and fluctuate thermodynamically. If all the exchange interactions were positive, there would be ferromagnetic phase transition at a finite temperature, below

which the system falls into one of the two global minima of the free energy, namely, the ordered states. Frustration of the interactions drastically changes the situation. Generally, spin glasses are random magnetic systems, with competing interactions . Here, frustration in the context of spin glasses arises due to the competition between ferromagnetic and antiferromagnetic quenched random interactions. Therefore, it is not possible for the spins to energetically satisfy every bond associated with them simultaneously. In the spin glass phase , frustration induce large energy barriers between states that are closely spaced in energy. This leads to very long relaxation times and the occurrence of spontaneous cooperative freezing of the (random) spin orientations. The random interactions generate many local minima in the free energy landscape, each of which may represent a seemingly random configuration of the spins. However, the spins may be frozen into such a configuration at low temperatures : this spin freezing is the essence of the spin glass order. Each interaction coupling J_{ij} is expected to be distributed independently according to the probability distribution($P(J_{ij})$). We can use the Gaussian or the bimodal as typical examples of the distribution of $P(J_{ij})$. The mathematical expressions of the two distributions are:

$$P(J_{ij}) = \frac{1}{\sqrt{2\pi J^2}} \exp(-\frac{(J_{ij} - J_0)^2}{2J^2}), \tag{2.3.2}$$

$$P(J_{ij}) = p\delta(J_{ij} - J) + (1 - p)\delta(J_{ij} + J), \tag{2.3.3}$$

respectively. From the above equations eq.(2.3.2) is a Gaussian distribution with mean J_0 and variance J^2, while in the eq.(2.3.3) J is either $J(> 0)$ (with probability p) or -J(with probability 1-p)[56]. Depending up on the the specific problem the nature of randomness in interaction coupling (J_{ij}) has different types of origin. For

instance, in some spin glass materials, the positions of atoms carrying spins are randomly distributed, hence the randomness is the consequence of these interactions[38]. Therefore, for such a kind of systems it is very difficult to identify the location of each atom precisely. Then just to find the locations of the atom, we have to introduce the probability distribution for J_{ij}. Thus, J is supposed to be distributed randomly and independently at each site(ij) according to the probabilities above. In this thesis we will concentrate on a generalization of the Edwards- Anderson Ising spin glass model, in which the bonds take only two values $J_{ij} = \pm 1$, with equal probability and the probability that two spins are linked by a bond depends on the distance between the two spins . A theoretical measure of the spin-glass phase is called the overlap order parameter[49]. To define it, we duplicate the random exchange interaction in equation(2.3.1) and change the Hamiltonian to:-

$$H = -\sum_{\alpha,\beta=1,2}\sum_{\langle ij\rangle} J_{ij}\sigma_i^{(\alpha)}\sigma_j^{(\beta)}, \tag{2.3.4}$$

where the superscript of the spin variables indicates each replica of the system. The spins of one replica and those of the other are thermodynamically independent. Nonetheless, we can expect that the spin configurations of the two replicas are similar to each other at low temperatures, if there is a single thermodynamic state into which the system is frozen else the overlap can take different values (including zero) if many different states are present. Thus, we define the order parameter as the hamming distance of the spin configurations of the replicas[49]. For a given instance J of the quenched disorder the overlap is defined as

$$q_J^{\alpha\beta} = \frac{1}{N}\sum_{i=1}^{N}\langle\sigma_i^{(1)}\rangle_\alpha\langle\sigma_i^{(2)}\rangle_\beta. \tag{2.3.5}$$

where $\langle ... \rangle_\alpha$ is thermal average in the state α. Here N is the number of lattice sites. One may regard that the two replicas represent the same system at two moments in time with infinite interval[44]. The self-overlap, also called Edwards- Anderson parameter is defined as

$$q_{EA} = \frac{1}{N} \sum_{i=1} \overline{\langle \sigma_i \rangle^2}. \tag{2.3.6}$$

Where the over bar denotes average over J_{ij} realizations. Varying instance of disorder, the values of q_J fluctuate. The order parameter of the spin-glass phase is the overlap distribution function averaged over the probability distribution of the distributed bonds.

2.3.1 Critical behavior

To calculate the phase transition temperature we have used the finite size scaling(FSS)property of the observable:

$$g = \frac{1}{2}(3 - \frac{\overline{\langle q^4 \rangle}}{\overline{(\langle q^2 \rangle)^2}}), \tag{2.3.7}$$

called Binder parameter (Binder cumulant). Here $\langle ... \rangle$ refers to the average over the thermodynamical ensemble, while the over bar represents the mean over the random distribution of the interaction couplings (bonds). The overlap parameter q as we have defined, for numerical computation, as:

$$q = \sum_i \sigma_i^{(1)} \sigma_i^{(2)}, \tag{2.3.8}$$

where the upper index is the real replicas or identical copies. The finite size scaling form of the Binder parameter is:

$$g = \overline{g}(N^{\frac{1}{\nu}}(T - T_c)), \tag{2.3.9}$$

where N is the total size of the system. Since at $T = T_c$, for every size, is g =g(0), the critical temperature can be obtained from different sizes g(T) intersections. To calculate this parameter, we have considered the scaling behavior of the critical temperature for a finite size system:

$$T_c(N) - T_c^{\infty} = BN^{-\theta}, \tag{2.3.10}$$

where the T(N) is a point where the intersection between the g(T) for the size N/2 and the g(T) for the size N and $\theta = \frac{1}{\nu}$ [60].

2.3.2 Distance dependent interaction coupling

In this part of the dissertation we explore distance dependent interaction coupling in 2D in order to show how a phase transition arises when couplings between far away spins are permitted. We consider the following Hamiltonian:-

$$H = -\sum_{ij} J_{(i<j)} s_i s_j. \tag{2.3.11}$$

The interaction coupling is a quenched random variable whose probability of being non-zero decays with distance between two spin sites[61, 62]. That means, if we have two spins s_i and s_j, and the distance between them is $r_{ij} = |i - j|$. The probability distribution of the existence of an interaction coupling can be written as

$$P[J_{ij} \neq 0] \propto r_{ij}^{-\rho}, \tag{2.3.12}$$

for $r_{ij} \gg 1$. The probability of the non zero interaction coupling is equal and the bond distribution is Gaussian with zero mean and variance($\overline{J_{ij}^2} \propto r_{ij}^{-\rho}$). The spin glass models with power-low decaying interactions actually allow to study long and short

range regimes by changing the power (ρ)[61]. Therefore, here ρ plays a key role to simulate different statistical mechanical behaviors.

We know that some physical quantities diverge seemingly to infinity at the critical point. The divergence is, strictly speaking, only in the thermodynamic limit that $N \to \infty$, where N is the number of degrees of freedom. This raises a challenge for numerical simulations to see the critical phenomena since we have to simulate systems at different sizes.

In the model, we study changing of ρ among three different regimes. As ρ is large the power-law is decaying rapidly and only bonds with neighboring site are plausible. We study the 2D case, in which no spin glass transition exists and the interactions are short-range. But when the value of ρ is not large, there is a probability to get interaction coupling. We can check the existence of spin glass phase for $\rho < 2D$ where the system critical behavior starts being long-range rather than short-range . For $\frac{4}{3}D < \rho < 2D$ there will be a phase transition but the system is out of the range of the validity of mean-field theory. Therefore, to probe the critical behavior one must resort to other approaches . One useful approach is numerical simulation, that is the theme of the present part of this dissertation. As $\rho < \frac{4}{3}D$ there critical behavior is mean-field like with critical exponents $\nu = \frac{1}{\rho - D}$ and $\eta = D - 2 - \rho$. To summarize this for 2D system:

$\rho > 4(2D)$ no phase transition

$2.67(\frac{4}{3}D) < \rho < 4(2D)$ phase transition but not mean-field

$\rho < 2.67(\frac{4}{3}D)$ mean-field critical behavior

2.4 Results and Discussion

As explained above in this part of the thesis we considered the Edwards-Anderson spin glass model in 2D, with random couplings and zero external magnetic field in periodic boundary conditions. We used the parallel tempering(PT) Monte Carlo algorithm, in order to escape from free energy landscapes that have many local minima and to reduce relaxation time for low temperature regions. In the parallel tempering Monte Carlo algorithm[45, 63, 64, 65], we simulated different systems at different lattice sizes(table 2.1).

Table 2.1: parameters we used for the simulation

Rho (ρ)	Lattice size(L)	No. of samples (NJ) (MCS)	No. of Monte Carlo steps (M)	No. of temperatures	ΔT (*change* in T)
2	10,20,30,40	200(for small L)& 100(for large L)	100000	10	0.2& 0.1
3	10,20,30,40	200(for small L)& 100(for large L)	500000	10(for small L)& 20(for large L)	0.2 & 0.1
4	10,20,30,40	200(for small L)& 100(for large L)	1000000	10(for small L)& 20(for large L)	0.2& 0.1

But the common belief is that there is no finite temperature phase transition for the two dimensional systems studied here. Hence, in both the bimodal spin glass and Gaussian spin glass, we expect the Edwards-Anderson order parameter as a function of temperature to be zero for all temperatures. Therefore, in order to show the phase transition, we implemented a diluted version of distance dependent interaction with decaying in probability as an inverse power of the distance. In such a kind of model

we can vary the power to change the dimension in short-range models and the model helped us to study the spin glass phase in and out of the range of validity of the mean field regime[61]. An average coordination number that we have used in the simulation is Z= 6.

The bonds are computed according to the following algorithm:

1.Compute the distance r between two randomly selected lattice sites i and j.

2. Compute the probability $w_{ij} = \frac{r_{ij}^{-\rho}}{\sum_{r=1}^{max} r_{ij}^{-\rho}}$ where $\sum_{r=1}^{max}$ is the sum over all possible values of distance r in the square 2D lattice with periodic boundary conditions.

3. Extract a random number between 0 and 1, if it is less than w_{ij}, there is a bond between i and j . Points 1 to 3 are repeated $N \times Z$, where Z is the average coordination number. Fig.2.1 is the comparison between the relaxation time of standard Monte

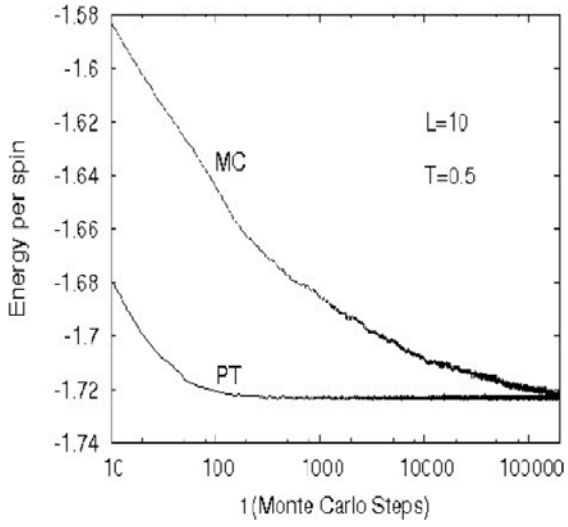

Figure 2.1: *Schematic representation of Energy per spin versus t(Monte Carlo steps) for L=10 and T=0.5, in this case the energy at a standard Monte Carlo algorithm compared with the energy at the same T obtained with the PT algorithm.*

Carlo and parallel tempering Monte Carlo simulations. The figure clearly indicates that the parallel tempering Monte Carlo method increases the speed of relaxation to equilibrium in the simulation. Fig.2.2 and fig.2.3 are presented to compare energy per

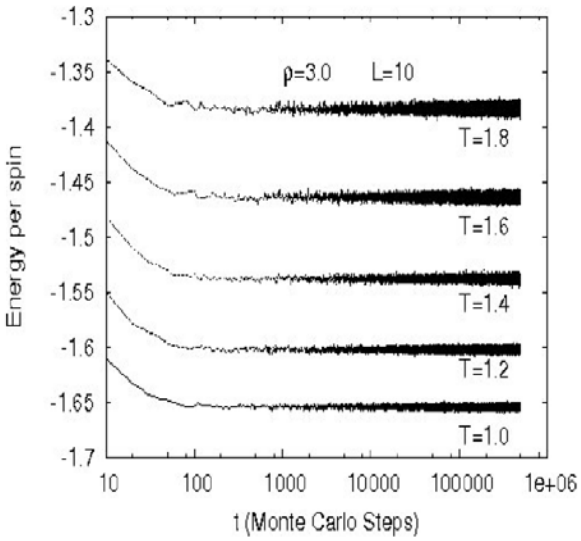

Figure 2.2: *Schematic representation of Energy per spin versus t(Monte Carlo steps) for* $\rho = 3.0, L = 10, T = 1.0, 1.2, 1.4, 1.6, 1.8$.

spin versus Monte Carlo steps for $\rho = 3.0$ and $\rho = 4.0$. In both cases the systems are thermalized but as ρ increases the existence of interaction coupling between distant spins is decreasing so that this reduces the simulation time. In fig.2.4 and fig.2.5 we look at the probability distribution, averaged over disorder, of the overlap. To this aim at each temperature we have simulated two copies of the system independently. At the high temperature, paramagnetic phase will appear with a zero overlap, i.e. a $p(q) = \sigma(q)$, where $\sigma(q)$ is Dirac delta function. As the sizes of the system are finite there should be a sharp peak in the thermodynamic limit appears as a broaden,

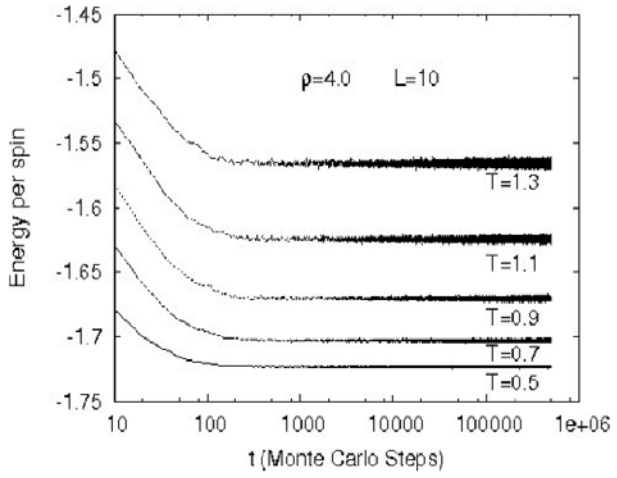

Figure 2.3: *Schematic representation of Energy per spin versus t(Monte Carlo steps) for* $\rho = 4.0, L = 10, T = 0.5, 0.7, 0.9, 1.1, 1.3$.

Gaussian, distribution whose variance decreases with size (see fig.2.4 T= 2.8 at $\rho = 3.0$ and fig.2.5 T =2.4 at $\rho = 4$). When the temperature is becoming lower and lower the size of the peak is also becoming wider and wider at some lower critical temperature there is a spin glass phase transition and p(q) is distributed symmetrically about zero in the interval $[-q; q]$ and displays a double peak. Here we performed the parallel tempering Monte Carlo simulation for $\rho = 2; 3; 4$. On the bases of the observation of the shape of the p(q) for different sizes we can determine that

- at $\rho = 2$, $T_c \sim 2$
- at $\rho = 3$, $T_c \sim 1.7$
- at $\rho = 4$, $(T_{10} \sim 1.6, T_{20} \sim 1.5, T_{30} \sim 1.3, T_{40} \sim 1.2$

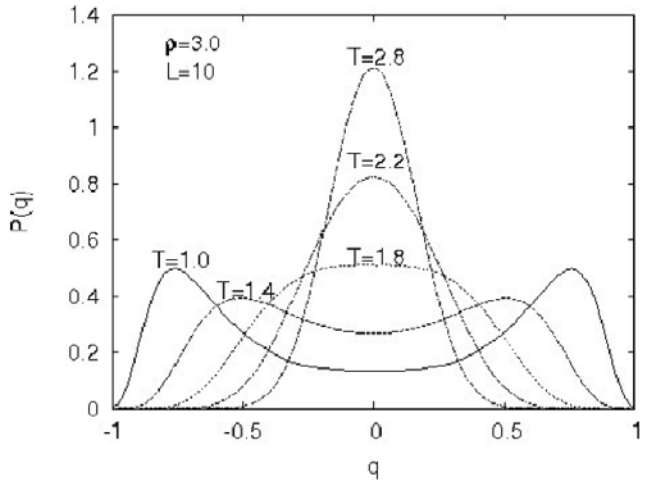

Figure 2.4: *The plot of P(q) versus q for different temperatures* ($T = 1.0; 1.4; 1.8; 2.2; 2.8$)$\rho = 3.0, L = 10$. *Thefigure explains how pure paramagnetic phase is translated to spin glass phase depending on temperature.*

It is evident that, at high temperatures p(q) is narrow (bell) shaped. For temperature going to infinity the shape of p(q)will approach to a delta function. For temperatures lower than spin glass phase transition temperatures, p(q) exhibits a symmetric two peak structure with the maximum values of the function shifts to $q = \pm 1$ fig.2.6 clearly shows that the probability distribution of overlap parameter depends on the system size. This means that the larger the system size the higher the peaks of the p(q) and the faster the thermalization. In fig.2.7 also as we mentioned above the peaks of p(q) depends on system size and temperature. This implies that the thermalization time grows enormously as the temperature is progressively decreased. Fig.2.8 explains about the Binder parameter which is very important parameter to identify the critical temperature. In this case as we have seen from section

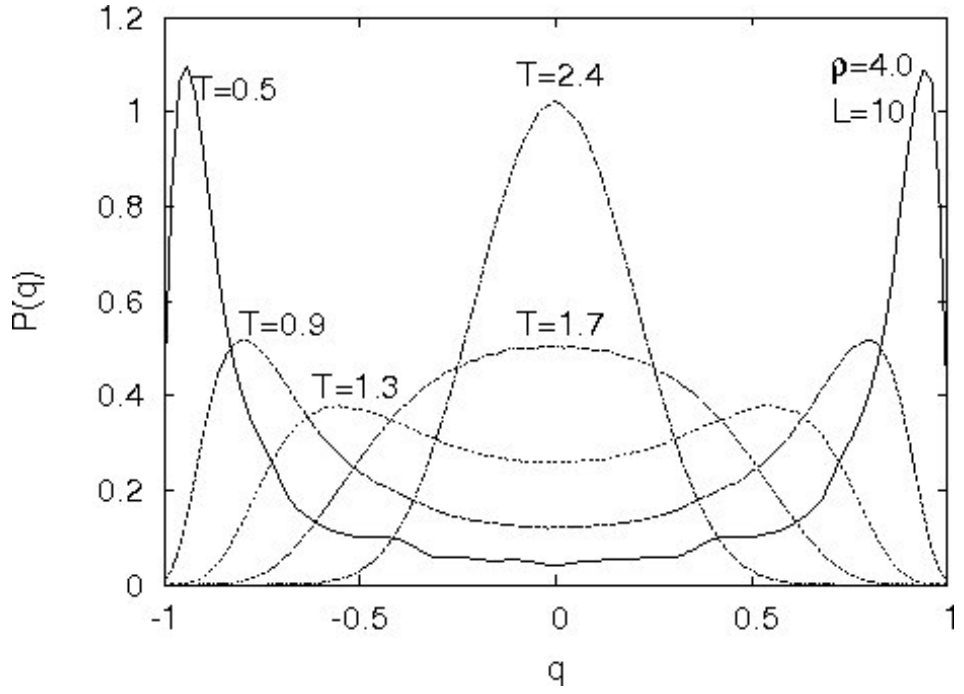

Figure 2.5: the plot of P(q) versus q for different temperatures $\rho = 4.0$, $L = 10$, $T = 0.5, 0.9, 1.3, 1.7, 2.4$. In this case, the figure shows how the peaks of p(q) depends on the value of ρ and temperature.

2.3, the intersection point of the curves of Binder parameter versus temperature for different system sizes indicate the transition temperature. We attached some of the figures for different system sizes and values of rho in A.1 for further comparison.

2.5 Conclusions

This part of the thesis reports the results of Monte Carlo simulation of two dimensional spin glass systems with distance dependent interaction. We have considered two dimensional Ising spin glass model. In this case since the system is disordered system, we have free energy land escapes. To overcome the energy land escapes and

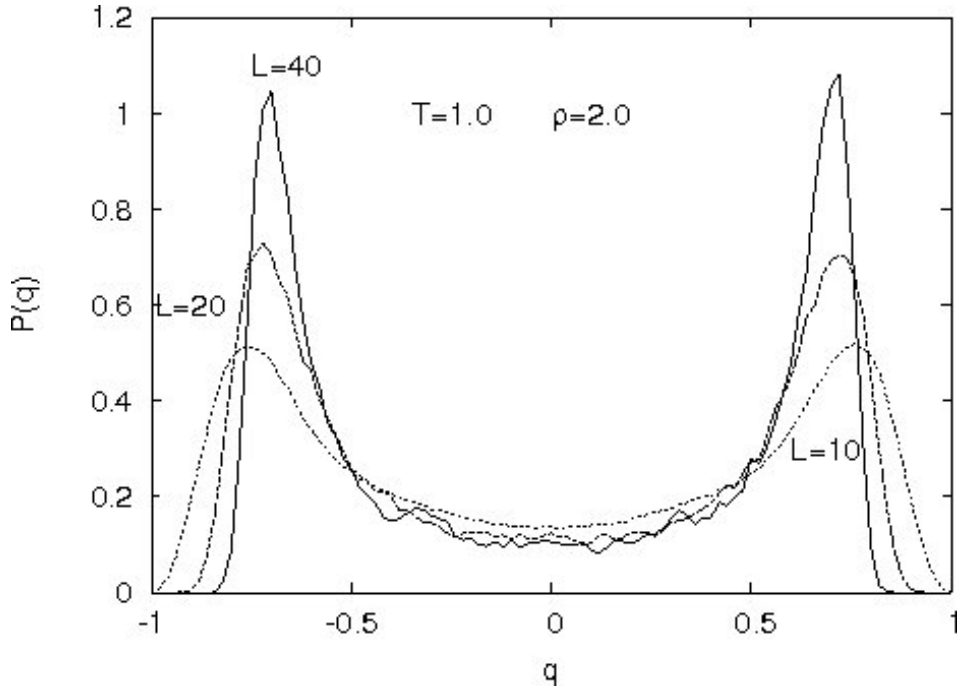

Figure 2.6: the plot of P(q) versus q for different system sizes ($L = 10, 20, 40$) and $\rho = 2.0, T = 1.0$. The figure clearly shows that how the value of p(q) depends on system size.

to minimize the relaxation time of the simulation we implemented the parallel tempering Monte Carlo simulation .The model does not provide any phase transition for nearest neighbor interactions. This is consistent with the present spin glass theory. In order to show the spin glass phase transition we considered the long-range interaction model i.e. diluted version of power low decaying interaction coupling. The model that we considered is a diluted version, i.e. , every spin is connected with a finite number of other spins so that we have chosen an average coordination number z=6. The results that we obtained are summarized as follows:

1.The parallel tempering Monte Carlo simulation reduces the relaxation time and

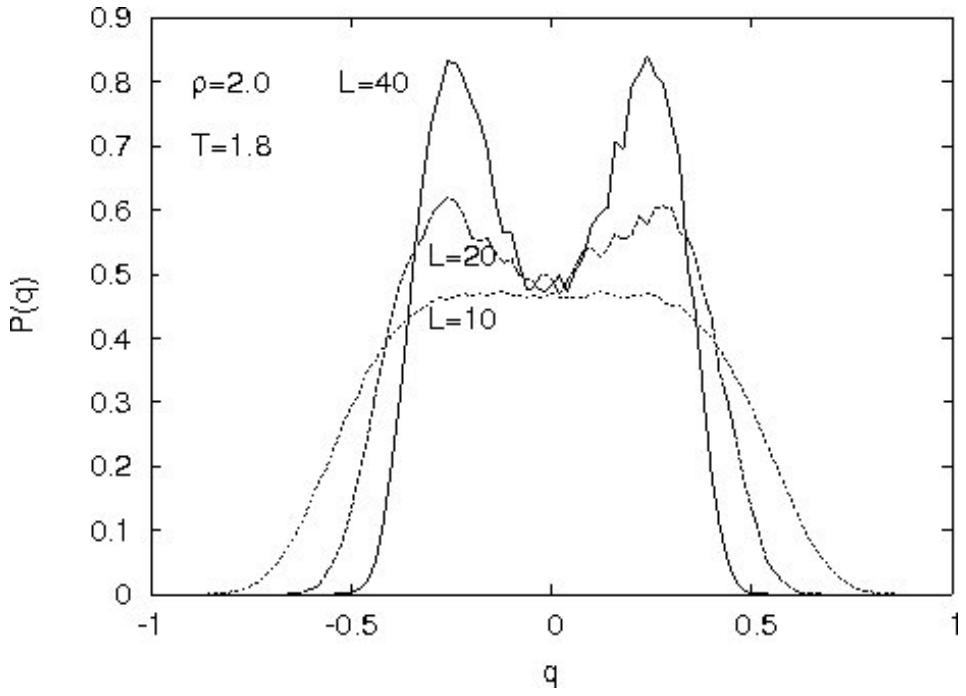

Figure 2.7: the plot of P(q) versus q for different system sizes($L = 10, 20, 40$) $\rho = 2.0, T = 1.0$

speed up the equilibration of the simulation and all data that we have shown are thermalized.

2. We have simulated different systems with different geometrical organization of random interactions. For each system we have simulated two replicas in order to study the overlap order parameter.

3. We have computed the overlap distribution function for $\rho = 2; 3; 4$. In the first two cases we found evidence for the existence of a phase transition from the paramagnetic to the spin glass phase. In the last case, double peaked distributions, typical of the spin glass phase are displayed at low T for small sizes. However, the T_c at which the conversion from single peak in to double peak occurs, appear to

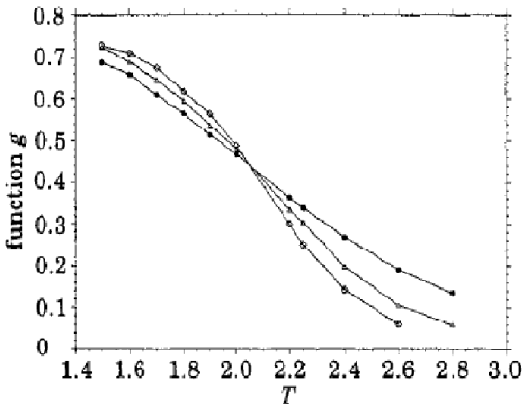

Figure 2.8: *The plot of Binder parameter versus Temperature for different system sizes(L= 10;20;40)* $\rho = 2.0$

continuously decrease with L. This is in agreement with the fact that the value $\rho = 4.0$ indicates the cross over at which long-range systems whose interaction decrease with $r^{-\rho}$ becomes effectively short range. Since in 2D the short-range spin glass does not exist,T_c must go to zero in the proximity of $\rho = 4$.

Chapter 3

Heisenberg (Vector)spin model

This chapter deals with spin glass phase by extending the component of spins from one(Ising spin) to three(Heisenberg spin) model.

3.1 Introduction

The original spin glasses consisted of alloys containing three component vectorial localized spins and so are Heisenberg rather than Ising, with the magnetic impurities distributed at random in a non-magnetic metallic host. Typical alloys of this class are AuFe, CuMn, AgMn, AuMn, AuCr, ... with impurity concentrations of the order of a few percent. Experimentally these systems clearly have well defined spin glass transition temperatures of a few degrees per percent impurity. Spontaneous anti-alignment or alignment of molecular moments in antiferromagnets or ferromagnets implies the presence of an internal field. This field is known as the molecular field. In 1928, Heisenberg explained that the molecular field responsible for the magnetic ordering in solids is the consequence of a spin dependent interaction between moments on neighboring lattice sites. Furthermore, he considered that the exchange (potential)

energy between spin S_i and S_j on neighboring sites is given by,

$$V_{ij} = J_{ij}\vec{S_i}.\vec{S_j}, \tag{3.1.1}$$

where J_{ij} is the exchange interaction and spin S_i,

$$S_i = \frac{\hbar}{2}\sigma_i, \tag{3.1.2}$$

with σ_i being the Pauli spin matrices. As a result, for $J_{ij} > 0$ the lowest energy configuration is when the spins are aligned anti-parallel to one another, which leads to antiferromagnetic ordering of the magnetic moments. On the other hand, where $J_{ij} < 0$, the minimum energy configuration occurs when the moments are aligned parallel to one another, resulting in a ferromagnetic ordering of the moments.

The Heisenberg spin model consists of a Hamiltonian for an array of magnetic moments (spins) with the exchange interaction energy given in above. That is, the exchange interaction between all spins on the lattice point contributes the term in Eq. (3.3.1) to the Hamiltonian. Therefore this is a many-body Hamiltonian due to the large number of exchange interactions that must be considered (i.e. there are on the order of 10^{23} moments). The Heisenberg Hamiltonian for the two spin system is given above. Where S_i and S_j are spin-$\frac{1}{2}$ operators.

Exchange interactions decay rapidly with increasing distance; thus it is sufficient to only consider nearest neighbor exchange interactions. The term nearest neighbors means the moments which are physically closest to one another on a crystal lattice. For instance, the square lattice in figure below the pairs of moments at lattice sites 1 and 2 and at sites 1 and 3 are nearest neighbors pairs. If somebody asks, why the interaction couplings fall of rapidly with distance? the answer being that, it has to do with their underlying physical nature which means that interaction coupling between

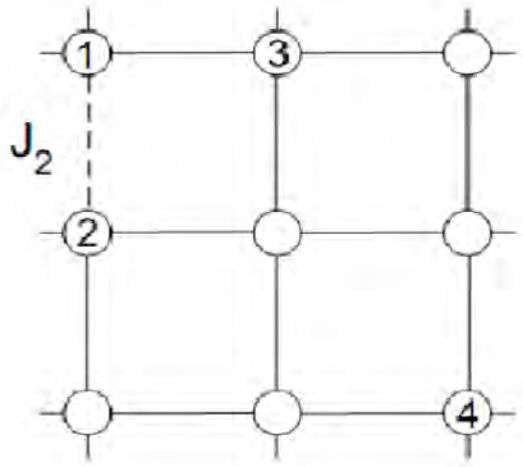

Figure 3.1: *Schematic representation of Spin-$\frac{1}{2}$ atoms situated on a square lattice. Atoms 1 and 3, and 1 and 2 are nearest neighbors*

electrons are spin-dependent forces arising from both Coulomb interactions and the Pauli Exclusion Principle, which they are subject too. The Coulomb force acts at a long range so that far apart electrons are influenced by one anothers electric field. The magnitude of the Coulomb repulsion depends on distance and varies as r^{-2}, where r is the distance between the electrons. However, for the Pauli Exclusion Principle to be a significant effect on a pair of electrons, they must be able to come very close to one another. Electrons whose wave functions have significant overlap, have the best chance of coming close to one another and thus the best chance of interacting via the Exclusion Principle. The wave function of electrons depend on the distance between the electrons (decays rapidly away from the electron). With few exceptions outer shell electrons in atoms 1 and 4, (see figure above), will have a smaller amount of overlap of

their wave functions compared with the overlap of electronic wave functions in nearest neighbor atoms 1 and 2. This leads to the conclusion that exchange interaction beyond those of the nearest neighbor type are relatively small, and can thus be neglected.

The origin of the exchange interaction energy is governed by the laws of quantum mechanics. Electrons usually interact via Coulombs law classically, and quantum mechanically via the Pauli Exclusion Principle. As we all know, the Pauli Exclusion Principle forbids electrons with like spins from coming close to one another which in effect reduces their coulomb repulsion. On the other hand, electrons with opposite spins can get close to one another resulting in a higher coulomb repulsion between them. The exchange energy can then be thought of as the difference in potential energy of the parallel and anti-parallel spin states. This spin dependent exchange energy is responsible for magnetic ordering in materials.

3.2 Spin glass phenomena

The basic parameters which indicate the properties of spin glass phase (state) are concentration of magnetic impurities, temperature and external magnetic field. External magnetic field is one of the parameters which might be interesting to investigate because it makes the spin align in the direction of the fields. The magnetic susceptibility is a response function of the system to the external magnetic field and provides information about the behavior of the system. Unlike ferromagnetic system in which the susceptibility exhibits a divergence at the critical temperature,in spin glass this parameter has a cusp which is considered as a prominent property of spin glass systems.

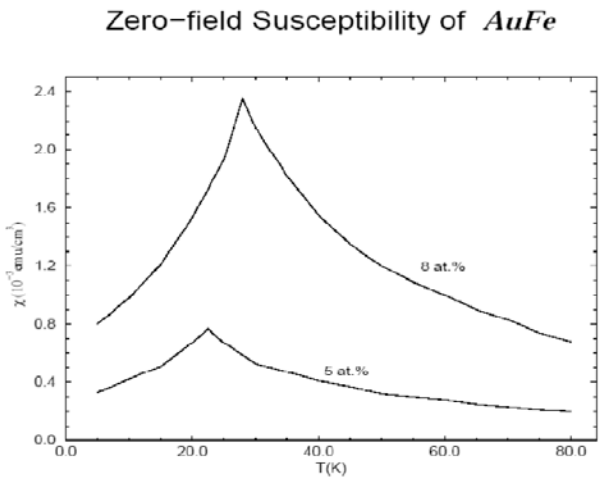

Figure 3.2: *Schematic representation of sharp pick (cusp) in the low-field susceptibility of low concentration AuFe alloys, from Cannella and Mydosh[48]*

3.3 Models of spin glasses in Heisenberg spin

For a Heisenberg spin glass in three dimensions, theoretical work appears to explain conclusively that there should be no ordering of the pure Edwards-Anderson type until zero temperature[67, 68, 69, 70]. On the other hand, experimentalists[71] clearly demonstrated that order at finite temperatures exists in these systems, at least under zero applied field. For Heisenberg spin model the spins interact through the Hamiltonian:

$$H = -\sum_{\langle ij \rangle} J_{ij} \vec{S}_i \cdot \vec{S}_j. \tag{3.3.1}$$

Where (ij) indicates a sum over nearest neighbors and the vector spin[87, 88] can be described as

$$\vec{S_i} \cdot \vec{S_j} = S_i^x S_j^x + S_i^y S_j^y + S_i^z S_j^z. \tag{3.3.2}$$

The vector spins $S_i, i = 1, ..., N$ have components $S_i^\alpha, \alpha = 1, ..., 3$ and are normalized in the unit sphere. The exchange constants or bonds (J_{ij}) are independent random variables drawn from a given distribution with mean zero and variance one. Which means that each exchange coupling (J_{ij}) is expected to be distributed as per the probability distribution $(p(J_{ij}))$. We use the Gaussian or the bimodal as typical examples of the distribution of $p(J_{ij})$ as mentioned in chapter two:

$$P(J_{ij}) = \frac{1}{\sqrt{2\pi J^2}} exp(-\frac{(J_{ij} - J_0)^2}{2J_0^2}), \tag{3.3.3}$$

$$P(J_{ij}) = p\delta(J_{ij} - J) + (1 - p)\delta(J_{ij} + J), \tag{3.3.4}$$

respectively. In eq. (3.3.4) J_{ij} is either $J(> 0)$ (with probability p) or -J(with probability 1-p)[49].

3.4 Finite size scaling method

It is obvious that, in all cases it is impossible to compute the critical exponents analytically. Therefore, to extract information about them, we can use numerical methods, such as Monte Carlo methods. In this case, the simulated systems must be finite, due to restricted capabilities of computers, and due to this they will not describe the thermodynamic limit. While scaling laws $G \propto |t|^{-x}$ are valid only for infinitely large systems, describing the critical behavior of finite systems leads to so

called finite size scaling[66, 55]. In the following, laws of the form

$$G(t, L) \propto L^{\frac{x}{\nu}} A(\frac{t}{t_0} L \frac{1}{\nu}), \tag{3.4.1}$$

will be defined as finite size scaling laws (FSS), with A being a universal scaling function but this function may be different for $t > 0$ and $t < 0$. However, in the limit $t \to 0$, A becomes a constant$A(0)$, and thus is the same for all values of L. In fact, this approach allows to estimate critical exponents by just finding the numerical values of the critical system on lattices with different extents L, and extracting $G(t = 0, L)$ as a function of L.

In the limit of reduced temperature ($t \to 0$) and size of the system ($L \to \infty$), the correlation length (ξ) of the infinite system will not be cut off by the size of the finite system any longer, and L can be replaced by the correlation length. Equation(3.4.1) then allows to reproduce the scaling laws of the infinite system. Substituting Eq. (2.2.4)into Eq. (3.4.1)yields

$$G(t = 0, L \to \infty) \propto L^{\frac{x}{\nu}} \approx \xi^{\frac{x}{\nu}} \propto |t|^{-x}. \tag{3.4.2}$$

Considering methods of real space re-normalization,we can determine finite size scaling laws from the singular part of the free energy density

$$f_s(t, h, L) = L^{-d} A(\frac{t}{t_0} L \frac{1}{\nu}, \frac{h}{h_0} L^{yh}), \tag{3.4.3}$$

where t_0 and h_0 are non-universal constants. The magnetic susceptibility χ, for instance, follows from:

$$\chi = \frac{\partial^2 f_s}{\partial h^2}|_{h=0} = L^{2yh-d} A_\chi(\frac{t}{t_0} L \frac{1}{\nu}) = L^{\frac{\gamma}{\nu}} A_\chi(\frac{t}{t_0} L \frac{1}{\nu}). \tag{3.4.4}$$

3.5 Parameters that indicate Spin Glass phase

According to Edwards and Anderson (1975) work the response function in the language of phase transition the order parameter can be defined as

$$q_{EA} = [\langle \sigma_i \rangle^2]_{av}, \tag{3.5.1}$$

where the curly bracket ($\langle ... \rangle$) denotes the thermal average and the square bracket ([...]) shows an average over random realization. Since the orientation of the spins is random over the distribution of site i, the overlap parameter $q_{EA} = 1$ at T=0 and $q_{EA} \to 0$ as $T \to T_{SG}$. If the system is infinite system in equilibrium state, every spin can give the same value of q_{EA}. But, if the system is finite system, the order parameter is likely to vary from one site to another. Therefore, in order to find reliable value of the overlap parameter of the spin glass phase, we have to compute average over all spins i.e.

$$q_{EA} = [\frac{1}{N} \sum_{i}^{N} \langle \sigma_i \rangle^2]_{av}. \tag{3.5.2}$$

Where $N = L \times L \times L$ is the volume and L is the linear lattice size. However, since our method is Monte Carlo method, we can replace the thermal average by time average:

$$q_{EA}(t) = [\frac{1}{N} \sum_{i}^{N} (\frac{1}{MCS} \sum_{\tau=0}^{t} \sigma_i(\tau))^2]_{av}, \tag{3.5.3}$$

or

$$q_{EA}(t) = [\frac{1}{N} \sum_{i}^{N} (\frac{1}{MCS^2} \sum_{\tau_1, \tau_2} \sigma_i(\tau_1)\sigma_i(\tau_2))]_{av}, \tag{3.5.4}$$

where MCS is the number of Monte Carlo steps in the sample. But the spins have different configurations, so that it is better to compute the two replicas(copies) with

the same bonds. Therefore the order parameter can be written as:-

$$q_{EA}(t) = [\frac{1}{N}\sum_{i}^{N}(\frac{1}{MCS}\sum_{\tau}\vec{\sigma}_i^{\alpha}(\tau)\cdot\vec{\sigma}_i^{\beta}(\tau))]_{av}. \tag{3.5.5}$$

Where σ_i^{α} and σ_i^{β} are the two replicas. For classical vector spins it can be defined as

$$q_{EA}(t) = [\frac{1}{N}\sum_{i}^{N}(\frac{1}{MCS}\sum_{\tau}\vec{\sigma}_i^{\alpha}(\tau)\cdot\vec{\sigma}_i^{\beta}(\tau))]_{av}. \tag{3.5.6}$$

It is possible to interchange the order of averaging in Monte Carlo simulation so that the above eq. can be written as:-

$$q_{EA}(t) = [\frac{1}{MCS}\sum_{i}^{N}(\frac{1}{N}\sum_{\tau}\vec{\sigma}_i^{\alpha}(\tau)\cdot\vec{\sigma}_i^{\beta}(\tau))]_{av}. \tag{3.5.7}$$

As we mentioned earlier the system is random so that no net tendency of ferromagnetism and antiferromagnetism, the spin correlation function $\langle\sigma_i\sigma_j\rangle$ can be either ferromagnetism or antiferromagnetism, based on the random distribution of exchange interaction. Therefore, to check the long-range order, we have to define the spin glass susceptibility

$$\chi_{SG} = \frac{1}{N}\sum_{ij}[\langle\sigma_i\sigma_j\rangle^2]_{av}, \tag{3.5.8}$$

that can diverge if the correlation length of the spins are larger than the lattice size(L). Calculation of spin glass susceptibility by using Monte Carlo simulation is not simple task. But, with a simple algebra, i.e. by using $\langle\sigma_i\sigma_j\rangle_T$ as $\frac{1}{MCS}\sum_t\sigma_i(t)\sigma_j(t)$ one can derive that

$$\chi_{SG} = \frac{1}{N}[(q_{corr}^2)_t]_{av}. \tag{3.5.9}$$

Where the quantity q_{corr} can be defined in the following way:

$$q_{corr} = \frac{1}{N}\sum_{i}\sigma_i(t_0)\sigma_j(t_0+t), \tag{3.5.10}$$

i.e. t stands for Monte Carlo time (steps). Our aim here is performing Monte Carlo simulation of the correlation function (q_{corr}), so that we have to take two identical copies of the system and allow them to evolve with time. Therefore, the procedure is based on the fact that sampling of (q_{corr}) the two replicas do not depend on the initial time so long as both parameters are already in equilibrium state, so that the above eq. can be written as:-

$$q_{corr}(t) = \frac{1}{N}\sum_{i=1}^{N} \sigma_i^{\alpha}(t_0 + t)\sigma_i^{\beta}(t_0 + t). \tag{3.5.11}$$

Where σ_i^{α} and σ_i^{β} are two identical copies (replicas) of classical vector spins. For our model, it is important to consider a quantity that is rotationally invariant in order to represent the fact that spins can rotate collectively. Therefore, in order to define spin glass susceptibility for this model, we have to define the order parameter in the following way:

$$Q = \sqrt{\frac{1}{3}\sum_{\alpha,\beta=1}^{3} (q^{\alpha\beta})^2}. \tag{3.5.12}$$

Where $q^{\alpha\beta}$ will be

$$q^{\alpha\beta} = \frac{1}{N}\sum_{i} \sigma_i^{\alpha}\sigma_i^{\beta}. \tag{3.5.13}$$

Another very important parameter that we use to determine the spin glass phase transition temperature is Binder parameter (Binder cumulant). The Binder parameter is a measure of the shape of the probability of the order parameter, and only looks at spatial averages (thus zero " momentum") so does not directly address the distance dependence of the correlation functions. As mentioned in chapter two, for the Ising system this parameter has the following form:

$$g_L = \frac{1}{2}[3 - \frac{\langle q^4 \rangle}{\langle q^2 \rangle^2}]. \tag{3.5.14}$$

But for Heisenberg spin model this parameter is defined as:

$$g_L = \frac{1}{2}[11 - 9\frac{\langle Q^4 \rangle}{\langle Q^2 \rangle^2}]. \tag{3.5.15}$$

We can say that g_L in this case to have a similar scaling property holds in Heisenberg system and thus provides a test for finite T_c. Binder parameter is a dimensionless quantity and the value of this parameter can be defined as:$0 \leq g_L \leq 1$. When the temperature $T \to \infty$, then the order parameter (Q) is a Gaussian distribution $g_L = 0$, and as at T=0 where Q is essentially a delta function (Q has a fixed value) $g_L = 1$. For an infinite system, g_L varies rapidly between this limit in the critical limit whereas at finite system this variation is slower. Here at T_c the correlation length becomes larger than the lattice size of the system and the Binder parameter has no size dependence. In general, the plot of Binder parameter vs temperature enables one to estimate the freezing temperature T_c as the curves of different sizes of the system should intersect at T_c[72, 73]. Therefore, g_L shows finite size scaling law as:-

$$g_L(L, T) \sim \tilde{g_L}(L^{\frac{1}{\nu}}(T - T_c)). \tag{3.5.16}$$

3.6 Numerical Techniques

The Monte Carlo simulation uses a multispin coding technique[74, 75, 76] in which each spin and bond is represented by a single bit of a computer word. For instance, on a 32 bit machine we then flip in parallel 32 spins (on the same lattice site but in different samples with different realizations of the disorder). Monte Carlo scheme is a stochastic method to determine physical quantity of a system which has many degrees of freedom. Therefore, here we considered 20,000 Monte Carlo steps (MCS), lattice size (L=5, 7, 10, 15, 20) and 100 realizations in order to calculate the physical quantities that indicate the spin glass phase.

3.7 Results and Discussion

In this part of the dissertation we considered the Edwards-Anderson spin glass model in 3D Heisenberg spin (vector spin), with random couplings and zero external magnetic field in periodic boundary conditions and obtained the following results

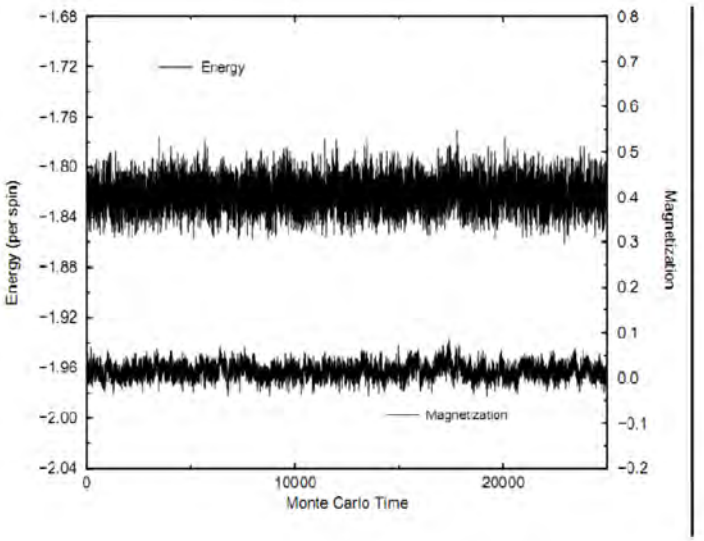

Figure 3.3: *Explains the relationship between Monte Carlo time steps with that of global energy and magnetization for lattice size (L=7). The figure shows that how internal energy and magnetization fluctuates from their average level for the specified lattice size.*

In fig.3.4 we plotted energy per spin vs. temperature for the mentioned lattice sizes but here there is no clear evidence of a size effect for energy which shows that lattice sizes are larger or comparable to the correlation length but this conclusion does not mean that other physical quantities may not show size dependence. Figure 3.5 indicates a plot of specific heat vs. temperature for various system sizes (L=7, 10, 15). As we can see from the figure there is a clear evidence of system size effect

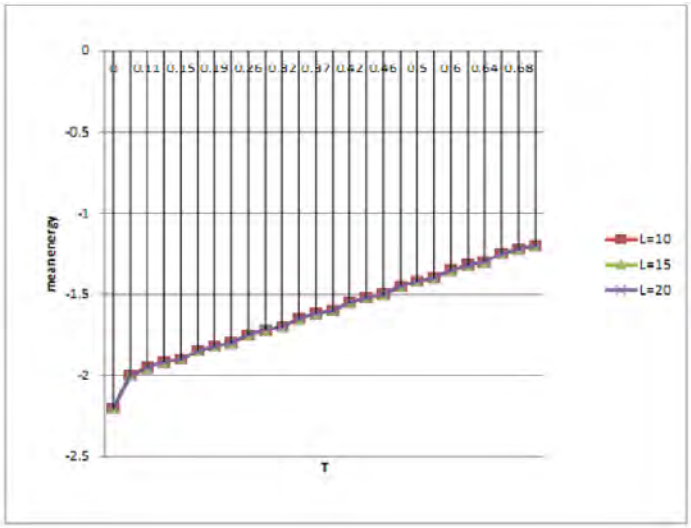

Figure 3.4: *Schematic representation of average energy versus temperature for system sizes(L=10, 15, 20)*

specially for small sizes but as the system size increases (L=10, 15) the effect is likely to reduce, which means as the system size increases the thermalization also increases. As explained above in section (3.5) of chapter three of this thesis, to say there is phase transition in the system, curves for different lattice sizes of Binder parameter vs. temperature must intersect at the transition temperature (T_c). Figure3.6 is a plot of Binder parameter vs. temperature for Heisenberg system of system sizes (L=5, 7, 10, 15, 20). As indicated the curves of several lattice sizes intersect nearly at $T_c \sim 0$ which means the system has no finite temperature phase transition.

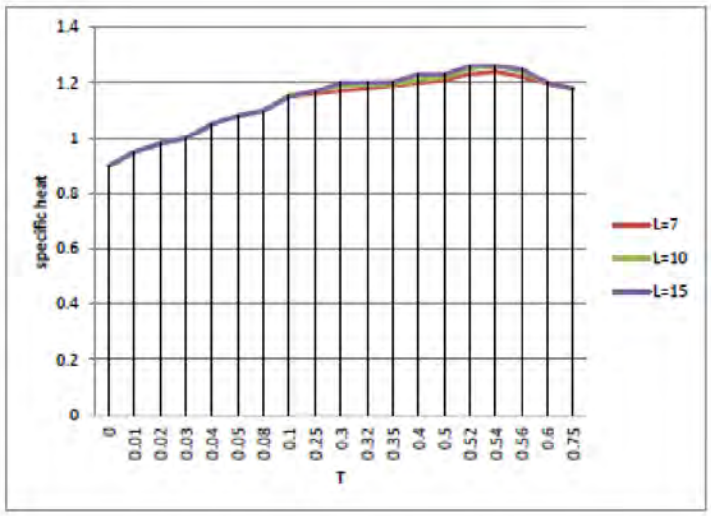

Figure 3.5: *Schematic representation of specific heat versus temperature for different system sizes (L=7, 10, 15).*

3.8 Conclusion

The idea of this work is to examine the stability of the spin glass phase in the Heisenberg model. We know that some physical quantities diverge seemingly to infinity at the critical point. This raises a problem for numerical simulations to see the critical phenomena since we have to simulate systems at different sizes and in order to address this problem we used the finite size scaling for the numerical simulation. Here, we used classical Heisenberg spin glass in 3D with the interaction following the Edwards-Anderson model and by using a plot of Binder parameter versus temperature for the curves of different system sizes we found the absence of finite temperature spin glass phase transition. When we examined non linear susceptibility also it appears that there is clear indication of the absence of finite temperature phase transition.

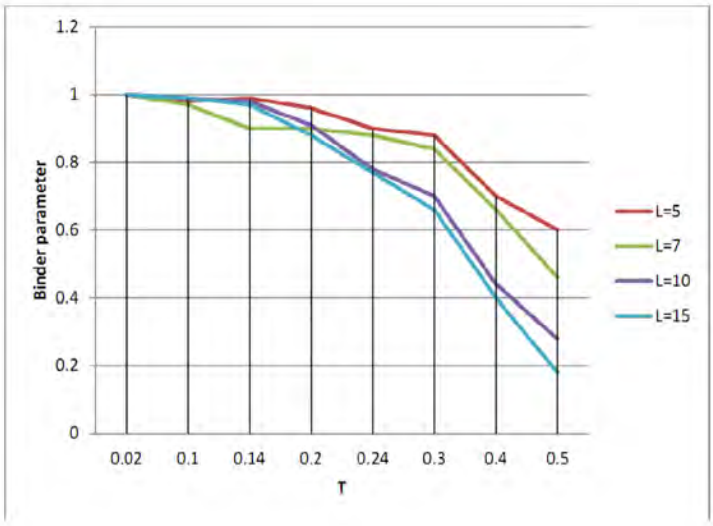

Figure 3.6: *Binder cumulant vs. temperature for lattice sizes(L=5, 7, 10, 15, 20).*

Chapter 4

Spin glass state in II-VI DMS at critical region using high temperature series expansion extrapolated with Padé approximants

In this part of the dissertation we study the magnetic properties of diluted magnetic semiconductors like magnetic susceptibility, correlation function, magnetic specific heat at the critical region by employing high temperature series expansion ($\beta \sim 0$)followed by Padé approximants. It is impossible to get exact solution for such kinds of many body system however these techniques give reliable results.

4.1 Introduction

Studying quantum spin systems is one of the most interesting and challenging problems of many body theory in condensed matter physics. Because of their intrinsic many-body quantum character it is very difficult to compute even simple quantities

like magnetic susceptibilities or specific heats in a straight forward fashion. However, there are by now a number of powerful approaches like exact diagonalization[77] ,quantum Monte Carlo[78], temperature density matrix renormalization[79, 80] or high temperature series expansion[81, 82] which yield the desired results. The aim of this part of the dissertation is to provide high temperature series data which can serve as an input for quick data analysis.

4.2 High-temperature series expansion

High-temperature series expansions are one of a power series expansion methods available to study quantum spin systems on a lattice such as Heisenberg, the Hubbard, or t-J model.The aim of a high-temperature series expansion is to calculate the power series

$$Q(\beta) = \sum_{i=0}^{N} I_p(i)\beta^i, \tag{4.2.1}$$

of a thermodynamic property $Q(\beta)$ in the inverse temperature $\beta = \frac{1}{k_B T}$ up to a chosen order N. In this equation I_p represents the expansion coefficient. Various methods to compute a high temperature series expansion exist, the goal of the first methods that were developed was to facilitate or simplify the manual calculation of the the above eq. (4.2.1)[83]. The availability of computers profoundly changed the approach to high-temperature series expansions and series expansions in general, and today's methods are tailored for a straightforward implementation on a computer. A series expansion that is well suited for a computer implementation and can be used for different types of expansions is the Linked-cluster expansion. In this chapter we demonstrate how it can be used to calculate a high temperature series expansion and

examine the requirements that a thermodynamic property has to satisfy the Linked-cluster expansion can be applied[84].

High-temperature series expansions can be conveniently represented by graphs and their expansions such as multigraphs(graphs that can have more than one edge between two vertices) and hypergraphs(graphs whose edge can connect more than two vertices). For instance, to define the square lattice spins Heisenberg Hamiltonian it is not sufficient to specify the position of spins in the lattice and the interaction term. In addition we have to identify the number of spins that can interact such as all nearest neighbor spins $\langle ij \rangle$ and the spin interaction can be represented by the Hamiltonian H_{ij} for a graph g. The definition of the model on the graph g will be:

$$H_g = -\sum_{ij\varepsilon g} H_{ij}. \tag{4.2.2}$$

Each vertex of the graph g corresponds to a site of the spins in the system and each edge represents an exchange interaction between the spins that can interact i.e. the interaction energy corresponds to H_{ij}. Now, let's consider the infinite graph of a quantum lattice model whose vertices are on the sites of a lattice and whose edges represent all interactions in the model. However, the models considered on the same lattice such as the square lattice may result in different lattice graphs as different sites of the lattice can interact. Thus the Heisenberg spins on the graph g

$$H_g = J\sum_{ij\varepsilon g} \vec{s_i} \cdot \vec{s_j}. \tag{4.2.3}$$

4.3 Linked-cluster expansion

Before presenting a detailed construction of the Linked-cluster expansion we briefly summarize the central result:If a linked cluster expansion for a property $Prop_g(\beta)$ for

a quantum lattice model on a finite graph g exists we later discuss the requirements that $Prop_g(\beta)$ has to satisfy. The $Prop_g(\beta)$ can be written as

$$Prop_g(\beta) = \sum_{C \subseteq g, Cconnected} Weigh_p(C, \beta). \tag{4.3.1}$$

Where the sum runs over all distinct connected subgraphs C of g. The weight $Weigh_p(C, \beta)$ of a graph, usually this refers to as a cluster, i.e. C is related with the inverse temperature β whose lowest order term is $\beta^{||C||}$, where $||C|| = |E(c)|$ is the number of edges(exchange interaction couplings) in C, and only depends on C but not on g. Thus only the weights of connected clusters with N edges or less have to be calculated to obtain $Prop_g(\beta)$ to order β^N and as we will later see also the thermodynamic limit of $P(\beta)$ on a lattice graph to order N. If the property $Prop_g$ only depends on the shape of the graph g then eq.(4.3.1) can be simplified to

$$Prop_g(\beta) = \sum_{C \subseteq g, Cconnected} (C.g) Weigh_p(C, \beta), \tag{4.3.2}$$

where the sum is over all different shapes of C that can be embedded into g and (C.g) counts the number of times C can be embedded into g. The weights themselves are calculated by inverting eq.(4.3.2) to

$$Weigh_p(g, \beta) = Prop_g(\beta) - \sum_{C \subset g, Cconnected} Weigh_p(C, \beta). \tag{4.3.3}$$

Starting with the smallest clusters and progressively going to larger clusters all weights can be constructed using eg.(4.3.3)

4.4 How to construct the linked cluster expansion

Now an explanation about a detailed construction of the linked cluster expansion of a thermodynamic property represented by $(Prop_g)$ of any quantum-lattice model

on a graph(vertices + edge) as defined by the Hamiltonian in Eq.(4.2.2)is presented. The methodology is based on a multivariable series expansion of the thermodynamic property ($Prop_g(\beta)$) (in formal expansion variables u_{ij} assigned to the edges ij of the graph g. These expansion variables guide us to assign the terms of the expansion to different subgraphs of g. The $Prop_g(\beta)$ is a function of the density matrix $\hat{\rho}_g(\beta)$ and we substitute βH_g by:

$$\beta H_g \rightarrow \sum_{ij\epsilon g} u_{ij} H_{ij}, \tag{4.4.1}$$

in the definition of density matrix. We consider such an assignment of variables or numbers to the edges and write $[u_{ij}]_g$. Here g can be dropped if the graph that is labeled is obvious from the context. By assuming $[u_{ij}] = \beta$ in our calculation we can obtain the thermodynamic value of ($Prop_g(\beta)$) and following this way at a later stage this leads us to rearrange the variables of the series in a useful way. Considering the substitution in Eq.(4.4.1) the density matrix and the thermodynamic property ($Prop_g$) become functions of the $[u_{ij}]$. Expanding $Prop_g([u_{ij}])$ in a multivariable series we get:

$$Prop_g([u_{ij}]) = \sum_{o_{ij}\geq 0} \alpha_{p,}[o_{ij}] \prod_{ij\epsilon g} (u_{ij})^{o_{ij}}, \tag{4.4.2}$$

here $[o_{ij}] > 0$ represents all integer labeling of the edges of g implies that $o_{ij} > 0$ for all $ij\epsilon g$. The expansion coefficients $\alpha_{p,}[o_{ij}]$ are explicitly given by

$$\alpha_{p,}[o_{ij}] = (\prod_{ij\epsilon g} \frac{1}{o_{ij}!} (\frac{\partial}{\partial u_{ij}})^{o_{ij}}) Prop_g([u_{ij}])|_{u_{ij}=0}. \tag{4.4.3}$$

Every edges of the graph $[o_{ij}]$, its expansion coefficient $\alpha_{p,}[o_{ij}]$, or term $\alpha_{p,}[o_{ij}] \prod (u_{ij})^{o_{ij}}$ can be identified as a multigraph by using o_{ij} edges between vertex i and j. An integer labeling or edge of the graph $[o_{ij}]_g$ introduces a subgraph g' of g by taking all edges with $o_{ij} > 0$ and avoiding all isolated vertices. By fixing the corresponding $[o_{ij}]_c$ for

the edges in g' also induces natural labeling $[o_{ij}]_{g'}$ of g'. The $Prop_g$ has to satisfy two basic requirements so that a linked cluster expansion can be constructed:

1.The expansion coefficient $\alpha_{p,}[o_{ij}]$ stated in Eq.(4.4.3) may only relay on the subgraph g' and the labeling $[o_{ij}]_{g'}$ induced by $[o_{ij}]_c$ with the exception of $[0]_g$, and this is a special case that incorporate the empty graph (for the time being we can consider that $\alpha_{p,}[0]_g = 0$. Then $\alpha_{p,}[o_{ij}]$ does not depend on the graph g in whose expansion it occurs, and once that we can calculate for one graph it can be used in the expansion of other graphs.

2.If the subgraph g' has more than one connected component $\alpha_{p,}[o_{ij}]$ must be zero . This leads to an expansion of $Prop_g$ in terms of connected subgraphs of g.

In this case in order to check the first requirement directly for a given property, a sufficient condition is that for any subgraph g' of g:

$$Prop_g([u_{ij}]_g)|_{u_{ij}=0 if ij \notin g'} = Prop_{g'}([u_{ij}]_{g'}). \tag{4.4.4}$$

Removing the interaction coupling (edge) from the density matrix avoids any contribution of the edge to the property. To check that the definition of the property in Eq.(4.4.4) is sufficient, we assume that we are given an integer labeling $[o_{ij}]_g$ with an induced subgraph C, and set g' in Eq.(4.4.4) equal to C. Then $\alpha_{p,}[o_{ij}]$ is an expansion coefficient of the series expansion of $Prop_C([u_{ij}]_C)$ and can thus only relay on the induced subgraph C. But this property is seldom mentioned it is essential if we want to reuse the expansion coefficients of a small graph for a larger one.

Now lets turn our attention to the second requirement: $\alpha_{p,}[o_{ij}]$ has to be zero if the subgraph induced by $[o_{ij}]$ has more than one connected component. A sufficient condition on $Prop_g$ is that for two disconnected graphs g_1 and g_2

$$Prop_{g_1 \cup g_2}(\beta) = Prop_{g_1}(\beta) + Prop_{g_2}(\beta). \tag{4.4.5}$$

Lets consider that the induced subgraph C of $[o_{ij}]_g$ consists of two disconnected components of graphs C_1 and C_2. Using the definition of $\alpha_{p,}[o_{ij}]$ in Eq.(4.4.3) for

$$Prop_{C_1 \cup C_2}([u_{ij}]_{C_1 \cup C_2}) = Prop_{C_1}([u_{ij}]_{C_1}) + Prop_{C_2}([u_{ij}]_{C_2}). \tag{4.4.6}$$

If we take partial derivative of the property for each u_{ij} of the induced subgraph $C_1 \cup C_2$, we can get that $\alpha_{p,}[o_{ij}]$ is zero, as derivatives of $Prop_{C_1}([u_{ij}]_{C_1})$ with respect to $u_{ij} \in C_2$ and derivatives of $Prop_{C_2}([u_{ij}]_{C_2})$ with respect to $u_{ij} \in C_1$ are taken on the right hand side of Eq.(4.4.6). Therefore only terms that have induced subgraphs which are connected have to be considered, giving the expansion method its name. Equation (4.4.5) is sometimes referred to as P being extensive but also holds for physically non extensive quantities such as two-point correlation functions.

While it is possible to perform a high-temperature series expansion using the connected multigraphs associated with the $\alpha_{p,}[o_{ij}]$, it is convenient to group the terms of Eq. (4.4.2) into weights assigned to the induced subgraphs. The weight $Weigh_p(C, \beta)$ of a subgraph C of g is the sum of all terms in Eq.(4.4.2) for which the subgraph induced by $[o_{ij}]$ is equal to C with all u_{ij} set equal to β. Writing $[o_{ij}] \to C$ for a $[o_{ij}]$ whose induced subgraph is equal to C the weight of a graph C is given by

$$Weigh_p(C, \beta) = \sum_{[o_{ij}] \to C} \alpha_{p,}[o_{ij}] \prod_{ij \in C} (\beta)^{o_{ij}}. \tag{4.4.7}$$

By construction the weight is independent of g and zero if C has two or more connected components. It uniquely assigns each of the terms of the multivariable expansion in Eq.(4.4.2) to a subgraph of g and $Prop_g(\beta)$ can be written as:

$$Prop_g(\beta) = \sum_{C \subseteq g, C connected} Weigh_p(C, \beta). \tag{4.4.8}$$

The weight defined by Eq. (4.4.7) has the following properties: By construction it is a polynomial in β whose lowest order contribution is of order $\beta^{||C||}$ because each edge $ij \in C$ has $o_{ij} > 1$ and thus contributes at least linearly in β. Furthermore the weight of a disconnected subgraph is zero by construction. To calculate the high-temperature series of $Prop_g(\beta)$ to order β^N with a connected-cluster expansion, it is thus sufficient to calculate the weights of all connected subgraphs of g with N edges or less. In Eq.(4.4.8) each connected subgraph C of g is uniquely defined by its location on g. Many properties and their weights will only depend on the shape of g and the subgraph C. Writing $(C \cdot g)$ for the number of times C can be embedded into g Eq.(4.4.8) simplifies to

$$Prop_g(\beta) = \sum_{C \subseteq g, Cconnected} (C \cdot g) Weigh_p(C, \beta) \tag{4.4.9}$$

The weight of a graph can be calculated by inverting Eq.(4.4.9) to:

$$Weigh_p(C, \beta) = Prop_g(\beta) - \sum_{C' \subseteq g, Cconnected} (C' \cdot C) Weigh_p(C', \beta). \tag{4.4.10}$$

Starting with small graphs and progressively going to larger graphs, we can calculate all the weights required for a particular calculation.

4.5 Procedures that can be used for the calculation of thermodynamic property

The determination of the high temperature series expansion of the thermodynamic property should be done in the following steps:

1.Determine all connected graphs g that can be embedded into the considered lattice.

2.Determine the property ($P_g(\beta)$) to order β^N for all graphs embedded:

3.Compute the subcluster counts ($C' \cdot C$).

4.Compute the weights of the property ($W_P(g,\beta)$) for all graphs using Eq.(4.4.10):

5.Determin the lattice counts L(C) for all graphs that considered.

6.Determin the high temperature series expansion of the property using Eq.(4.4.9).

4.6 Padé approximants (PA)

A mathematician named Henri Eugene *Padé* [1863-1953] used the method to approximate functions by rational functions and the method is called *Padé* approximants after him. However, this was not the first to use rational approximations, but he developed the theory more rigorously. One of the main applications of *Padé* approximations is to extract as much information as we can from a power series expansion that is known only for a few terms. Conversion from Taylor to *Padé* form usually accelerates convergence, and often allows good accuracy even out side of a power series' radius of convergence (which, incase of divergent asymptotic expansions, may be zero). He defined the theory as follows: took any series expansion of a function say $f(z) = \sum_{i=0}^{\infty} b_i z^i$ its $[L/K]$ *Padé* approximant is a rational function of the form:

$$[L/K] = \frac{c_0 + c_1 z + ... + c_L z^L}{a_0 + a_1 z + ... + a_K z^K}, \tag{4.6.1}$$

this fulfills

$$f(z) = \sum_{i=0}^{\infty} b_i z^i = \frac{c_0 + c_1 z + ... + c_L z^L}{a_0 + a_1 z + ... + a_K z^K} + O(z^{L+K+1}). \tag{4.6.2}$$

Equation(4.6.2) can be rewritten as:

$$(a_0 + a_1 z + ... + a_K z^K)(b_0 + b_1 z + ...) = c_0 + c_1 z + ... + c_L z^L. \tag{4.6.3}$$

As we can see in eq(4.6.1) the number of numerator coefficients are $L+1$ and the number of denominator coefficients are $K+1$. There is a more or less irrelevant common factor between them, and for definiteness we take $a_0 = 1$. Therefore, there are $L+1$ independent numerator coefficients but the denominator coefficients will reduce one component and will be K and making the total number of unknown $L+K+1$. This number suggests that normally $[L/K]$ ought to fit the power series in eq(4.6.1) through the orders $1, z, z^2, ..., z^{L+K}$. Equating the coefficients of $z^{L+1}, z^{L+2}, ..., z^{L+K}$ in equation (4.6.3), we get M equations where the unknown coefficients are $a_1, a_2, ...a_K$ (we recall that $a_0 = 1$). It follows immediately from (4.6.3) by equating the coefficients of $1, z, ..., z^L$ that:

$$c_0 = b_0, c_1 = b_1 + a_0 b_0, c_2 = b_2 + a_1 b_1 + a_2 b_0, ..., c_L = b_L + \sum_{i=1}^{min(L,K)} a_i b_{L-1}, \quad (4.6.4)$$

we find that

$$\begin{aligned} &a_K b_{L-K+1} + a_{K-1} b_{L-K+2} + ... + a_0 b_{L+1} = 0, \\ &a_K b_{L-K+2} + a_{K-1} b_{L-K+3} + ... + a_0 b_{L+2} = 0, \\ &. \\ &. \\ &. \\ &a_K b_L + a_{K-1} b_{L+1} + ... + a_0 b_{L+K} = 0. \end{aligned} \quad (4.6.5)$$

4.7 II-VI diluted magnetic semiconductors

There are several classes of semiconducting materials that are characterized by the random replacement of a fraction of the original atoms by magnetic atoms. The materials are usually known as diluted magnetic semiconductors (DMS) or semimagnetic semiconductors (SMSC).The first so-called diluted magnetic semiconductors (DMS) were II-VI semiconductor alloys like $Zn_{1-x}Mn_xTe$ and $Cd_{1-x}Mn_xTe$ [85]

originally studied in the 1980s. These materials are either spin glasses or have very low ferromagnetic (FM) critical temperatures T_c ($\sim$ $fewK$)[10] and are, therefore, inadequate for technological applications which would require FM order at room temperature. It's obvious that, the possibility of using the spin and the charge of the electrons for information processing will have numerous applications in recent technology and it is the basic theme of spintronics as mentioned above. The DMS materials can be considered as consisting of two interacting subsystems. The 1st one of these subsystems is the system of delocalized conduction or valence band electrons/holes. The 2nd one is the random and diluted system of localized magnetic moments associated with the magnetic atoms. These two subsystems interact with each other by the spin exchange interaction.

In this chapter, we study spin glass phase (state) that exists in II-VI semiconductors which consists of S, Te, Se, and of Zn, Cd. The fraction of cation sites are replaced with Mn (or Fe) as the magnetic impurity. A prototype of this is $Cd_{1-x}Mn_xTe$. Theoretical studies have shown that super exchange is the basic source of magnetic coupling, i.e., the filled valance band of the semiconductor exchange electrons with the half filled 3d band of the Mn. With this 2 electron process the interaction between the Mn will always lead to an antiferromagnetic orientation and seems to be true for both first and second nearest neighbors [10]. One of the advantages of II-VI materials is that they can host magnetic ions (e.g. Mn^{2+}) which open the way for studying various spin-dependent phenomena.

4.8 Models and interaction coupling calculations

We consider Heisenberg spin (vector spin) model with the Hamiltonian[**?**]:-

$$H = -2\sum_{ij} J_1 \vec{S_i} \cdot \vec{S_j} - 2\sum_{ik} J_2 \vec{S_i} \cdot \vec{S_k} - hg\mu_B \sum_i s_i^z, \tag{4.8.1}$$

Where (ij) and (ik) indicate nearest neighbors and next nearest neighbors summations respectively. The vector spin[87, 88] can be described as:-

$$\begin{aligned} \vec{S_i} \cdot \vec{S_j} &= S_i^x S_j^x + S_i^y S_j^y + S_i^z S_j^z, \\ \vec{S_i} \cdot \vec{S_k} &= S_i^x S_k^x + S_i^y S_k^y + S_i^z S_k^z. \end{aligned} \tag{4.8.2}$$

For diluted magnetic semiconductors containing the magnetic impurities[89] only in the octahedral sublattices, by using molecular-field approximation we can obtain the relationship between paramagnetic Curie-temperature (θ_p) and the Neel temperature (T_N), and the considered exchange interaction couplings J_1 and J_2. This method is according to Holland and Brown gives[90]:-

$$T_N = \frac{2s(s+1)}{3k_B}[-4J_1 + 2J_2], \tag{4.8.3}$$

and

$$\theta_p = \frac{2s(s+1)}{3k_B}[12J_1 + 6J_2]. \tag{4.8.4}$$

Where k_B is the Boltzmann's constant and $s = \frac{5}{2}$ is the spin of magnetic impurity (Mn^{2+}). Therefore, by using the experimental values of (θ_p) and T_N [91] we can determine the interaction couplings J_1 and J_2 for the concentrations ($0.6 \leq x \leq 1$). However, due to the nature of dilution problem in the system, we have to use the probability distribution to determine the interaction couplings for each concentration x ($0 \leq x \leq 1$). The probability of the occupation of the ions (i) can be defined as:-

$$P(i) = K_n^i x^{n-i}(1-x)^i. \tag{4.8.5}$$

Table 4.1: calculation of interaction couplings using magnetic measurements of (θ_p) and T_N

x	$T_N(K)$	$\theta_p(K)$	$\frac{J_1}{k_B}$	$\frac{J_2}{k_B}$
0.66	42	-548.75	-4.82	-6.04
0.70	48.81	-730	-6.26	-8.34
0.99	67	-925	-8.04	-10.34

Where n is the total number of lattice sites inside a sphere of radius (r_i) and its volume ($\frac{4}{3}r_i^3$) (r_i is the distance between ions i and j). Since, the structure of such system is a zinc blend structure, therefore n=12 and i varies from 0 to 12. The interaction coupling for such distribution (A or A') is assumed to be[92]:

$$J^i_{AA'} = (J_A^{n-i} J^i_{A'})^{\frac{1}{n}}. \tag{4.8.6}$$

Therefore, for the zinc blend structure we can define:

$$J^i_{AA'}(x) = \sum_{i=0}^{12} K^i_n x^{n-i}(1-x)^i (J_A^{n-i} J^i_{A'})^{\frac{1}{n}}. \tag{4.8.7}$$

When the interaction couplings $J_A(J_{A'})$ correspond to the nearest neighbor (nn), then $J^i_{AA'}(x) = J_1$. But if $J_A(J_{A'})$ corresponds to the next nearest neighbor (nnn), $J^i_{AA'}(x) = J_2$. Magnetic susceptibility is a measure of how fast the magnetization changes with a varying magnetic field. This quantity is important in our study because it is related to the exchange integrals of a system described in the Hamiltonian. Therefore, mathematically it can be defined as:

$$\chi = \frac{\partial M}{\partial h}, \tag{4.8.8}$$

where M and h stand for magnetization and magnetic field respectively. To identify the relationship between the two quantities, let's begin with the expression for the

zero field molar susceptibility for N atoms on a lattice[93],

$$\chi = N_A g\mu_B \frac{\partial}{\partial h} \langle \sum_i s_i^z \rangle |_{h=0}. \tag{4.8.9}$$

where N_A is Avogadros number. The notation χ will be used from here on to denote the molar susceptibility, unless otherwise stated. Taking the s_i to be spin-1/2 operators; the ground state expectation value (denoted by the angular brackets) is defined by,

$$\langle s_i^z \rangle = \frac{Tr(s_i^z e^{-\beta H})}{Tr(e^{-\beta H})}. \tag{4.8.10}$$

where Tr represents the trace (sum of the diagonal elements) of a matrix, and in this case H is the Hamiltonian. Differentiation of eq.(4.8.9) with respect to magnetic field yields:

$$\chi = \frac{N_A (g\mu_B)^2}{k_B T} \langle \sum_j s_i^z s_j^z \rangle |_{h=0}. \tag{4.8.11}$$

where k_B is the Boltzman constant. In order to expand the magnetic susceptibility by using High- Temperature Series Expansions, first we will find the relationship between susceptibility and correlation function i.e.

$$\chi(T) = \frac{N_A (g\mu_B)^2}{k_B T} \sum_{ij} \langle s_i \cdot s_j \rangle. \tag{4.8.12}$$

Here the spin correlation function can be defined as:

$$\langle s_i \cdot s_j \rangle = Tr(s_i s_j \hat{\rho}), \tag{4.8.13}$$

but $\hat{\rho}$ is spin density matrix. Here we seek to determine the density matrix ($\hat{\rho}$) using Lagrange multipliers and by maximizing the entropy(S)

$$S = -Tr(\hat{\rho} ln \hat{\rho}). \tag{4.8.14}$$

The change in the entropy corresponding to a small variation $\delta\hat{\rho}$ in the density matrix is approximately given by:

$$\delta S = -Tr[\frac{\partial}{\partial\hat{\rho}}(\hat{\rho}ln\hat{\rho})\delta\hat{\rho}], \tag{4.8.15}$$

or

$$\delta S = -Tr[(1 + ln\hat{\rho})\delta\hat{\rho}]. \tag{4.8.16}$$

Now, we maximize the entropy by setting $\delta S = 0$ and hence

$$Tr[(1 + ln\hat{\rho})\delta\hat{\rho}] = 0. \tag{4.8.17}$$

In addition, we note that

$$Tr(\lambda\hat{\rho}) = \lambda, \tag{4.8.18}$$

leads to

$$Tr(\lambda\delta\hat{\rho}) = 0. \tag{4.8.19}$$

with the aid of the expectation value of the Hamiltonian

$$\langle H\rangle = Tr(H\hat{\rho}), \tag{4.8.20}$$

one can write

$$Tr(\beta H\delta\hat{\rho}) = 0. \tag{4.8.21}$$

It is worth mentioning that λ and β are Lagrange multipliers. Now adding eqs(4.8.17),(4.8.19), and(4.8.21),we have

$$Tr[(1 + ln\hat{\rho} + \lambda + \beta H)\delta\hat{\rho}] = 0. \tag{4.8.22}$$

Since $\delta\hat{\rho}$ is quite arbitrary, we note that

$$ln\hat{\rho} = -(1 + \lambda + \beta H). \tag{4.8.23}$$

It then follows that

$$\hat{\rho} = e^{-(1+\lambda)} e^{-\beta H}, \tag{4.8.24}$$

so that application of the condition

$$Tr(\hat{\rho}) = 1, \tag{4.8.25}$$

leads to

$$e^{-(1+\lambda)} = \frac{1}{Tre^{-\beta H}}. \tag{4.8.26}$$

In view of this result, the expression for the density matrix takes the form

$$\hat{\rho} = \frac{e^{-\beta H}}{Tre^{-\beta H}}. \tag{4.8.27}$$

Therefore,the correlation function in between spins i and j will be

$$\langle s_i \cdot s_j \rangle = \frac{Tr(s_i s_j e^{-\beta H})}{Tr(e^{-\beta H})}. \tag{4.8.28}$$

And the magnetic susceptibility will be:

$$\chi(T) = (\frac{N_A(g\mu_B)^2}{k_B T}) \sum_{ij} \frac{Tr(s_i s_j e^{-\beta H})}{Tr(e^{-\beta H})}. \tag{4.8.29}$$

The solution of eq. (4.8.29) with the Hamiltonian given by eq. (4.8.1) has yet to be found. The main problem in finding a closed form solution is evident from the expression in eq.(4.8.28); it requires exponentiation of a Hamiltonian which is not diagonal. However, an approximate solution can be found for high temperatures, using a Taylor expansion of the exponential term. Letting i = 0 so that s_0^z is the reference spin (this can be any spin on the lattice), for high temperatures eq.(4.8.29) is:

$$\chi(T) = (\frac{N_A(g\mu_B)^2}{k_B T}) \sum_{j} \frac{Tr(s_0^z s_j^z (1 - \beta H + \frac{(\beta H)^2}{2!}) - \frac{(\beta H)^3}{3!} + ...)}{Tr(1 - \beta H + \frac{(\beta H)^2}{2!}) - \frac{(\beta H)^3}{3!} + ...)}, \tag{4.8.30}$$

where $\beta = \frac{1}{k_B T}$. Now, let's try to compute the coefficients in this expansion, albeit it turns out to be a difficult task for orders of β greater than one. considering only the lowest order term in this expansion, (i.e. β^0) eq.(4.8.30) becomes,

$$\chi(T) = (\frac{N_A(g\mu_B)^2}{k_B T}) \sum_j \frac{Tr(s_0^z s_j^z(1))}{Tr(1)}. \tag{4.8.31}$$

But the spins(s_0^z and s_j^z are spin-1/2 operators we have,

$$Tr(s_0^z s_j^z(1)) = \frac{1}{4}\delta_{0j} Tr(1), \tag{4.8.32}$$

where δ is the standard Kronecker delta notation. Therefore, eq. (4.8.31) can be compressed as $\frac{1}{4}Tr(1) \times (Tr(1))^{-1}$; because every term in the sum is zero except when j = 0. Finally, Tr(1) in both the numerator and denominator cancel out (note: $Tr(1) = 2^N$ where N is the number of lattice sites) and the susceptibility becomes,

$$\chi(T) = (\frac{N_A(g\mu_B)^2}{k_B T}) \frac{s(s+1)}{3}. \tag{4.8.33}$$

This eq.(4.8.33) is a Curie law ($\chi \sim 1/T$) explaining the susceptibility where the magnetic moments of the system are in disordered paramagnetic phase at high temperatures. Thus, if the magnetic susceptibility were valid for all temperatures (T), then the susceptibility would diverge as T approaches zero. But this assumption cannot be made from a mathematical stand point because the Taylor expansion itself is only valid for high T (small β). To get a better expression for the susceptibility of such systems, we have to consider higher order terms in the expansion. Now, let's try to see what will happen for β^1 terms are included in the expansion, then,

$$\chi(T) = (\frac{N_A(g\mu_B)^2}{k_B T}) \sum_j \frac{Tr(s_0^z s_j^z(1 - \beta H))}{Tr(1 - \beta H)}. \tag{4.8.34}$$

After some rearrangement we will get

$$\chi(T) = (\frac{N_A(g\mu_B)^2}{k_B T}) \sum_j \frac{Tr(s_0^z s_j^z) - \beta Tr((s_0^z s_j^z)(H))}{Tr(1) - \beta Tr(H)}. \tag{4.8.35}$$

However, no need to compute the first term in the numerator again since its expression is given by eq.(4.8.32). In addition that ,the denominator is only Tr(1) because Tr(H)=0. Therefore, we have to calculate the second term in the numerator only. Plugging eq.(4.8.1) in we get,

$$Tr((s_0 s_j)(H)) = J_1(\sum_R Tr(s_0^z s_j^z \hat{s_0} \cdot \hat{s_R})) + J_2(\sum_t Tr(s_0^z s_j^z \hat{s_0} \cdot \hat{s_t})). \tag{4.8.36}$$

Where $\hat{s_0} \cdot \hat{s_R} = (s_0^x s_R^x + s_0^y s_R^y + s_0^z s_R^z)$. Because different components of the spins are uncorrelated so that eq.(4.8.36)can be reduced to:

$$Tr((s_0 s_j)(H)) = \frac{1}{4}[1 - \frac{\beta}{4}(q_1 J_1 + q_2 J_2)]. \tag{4.8.37}$$

But in this expression q_1 and q_2 are the number of nearest neighbors (NN) and next nearest neighbors (NNN) respectively. By Plugging eq.(4.8.37) into (4.8.35) and after some simplifications, the magnetic susceptibility in its first order correction will be:

$$\chi = \frac{(\frac{N_A(g\mu_B)^2}{k_B T}\frac{s(s+1)}{3})}{T + (\frac{s(s+1)}{3k_B T})(q_1 J_1 + q_2 J_2)}. \tag{4.8.38}$$

Therefore this is the Neel's law of the form

$$\chi = \frac{C}{T + T_N} \tag{4.8.39}$$

where $C = (\frac{N_A(g\mu_B)^2}{k_B T})\frac{s(s+1)}{3}$ and $T_N = \frac{s(s+1)}{3k_B T})(q_1 J_1 + q_2 J_2)$.

Determination of the coefficients of higher order terms in the expansion, becomes increasingly difficult. Obviously, such difficulties arise for orders of β greater than 1 because of the Hamiltonian in the expansion terms becoming nonlinear, and terms having the form $Tr(s_0^z s_j^z H^2)$ must be computed. The aim of the calculation of coefficients for the higher order terms is to determine the relationship between the susceptibility and the exchange integrals J_1 and J_2. The coefficients for β^0 does not

reveal this relationship; however keeping more terms in the series expansion does. The expansion coefficients for β^1 , in equation (4.8.38), indicants that the susceptibility is a function of the exchange integrals. In effect, we have created a power series representation for $\chi * k_B T$ in powers of β,

$$\chi * k_B T = \sum_n \frac{1}{n!} \alpha_n (J_1 J_2) \beta^n. \tag{4.8.40}$$

As we have seen above, we found for n=0 and n=1 as follows:

$$\alpha_0 = N_A (g\mu_B)^2 \frac{s(s+1)}{3}, \tag{4.8.41}$$

and

$$\alpha_1 = N_A (g\mu_B)^2 (q_1 J_1 + q_2 J_2) (\frac{s(s+1)}{3})^2. \tag{4.8.42}$$

And magnetic specific heat of the system can be defined as:

$$c(T) = \frac{d\langle H \rangle}{dT} = \frac{1}{N} \frac{d}{dT} (\frac{Tr(He^{-\beta H})}{Tr(e^{-\beta H})}) = \frac{1}{N} \frac{d}{dT} (\frac{-\frac{d}{d\beta} Tr(e^{-\beta H})}{Tr(e^{-\beta H})}). \tag{4.8.43}$$

Expansions of the correlation function in powers of β and obtained as follows:

$$\langle s_i \cdot s_j \rangle = \frac{Tr(s_i s_j e^{-\beta H})}{Tr(e^{-\beta H})} = \sum_{l=0}^{\infty} \frac{(-1)^l}{l!} \alpha_l \beta^l. \tag{4.8.44}$$

According to the concept of linked cluster expansion $\alpha_l = \nu_l - \sum_{k=0}^{l-1} C_k^l \alpha_k \mu_{l-k}$, $\nu_l = \langle S_i \cdot S_j H^l \rangle$, and $\mu_m = \langle H^m \rangle$ the calculation of α_l leads to a diagrammatic representation according to [94]. This can be done by using two basic steps:

1. Identifying and cataloguing of all diagrams or graphs which can be constructed from one dashed line connecting the site i and j , and l straight lines, and the determination of diagrams whose contribution is none vanishing. This step has already been accomplished in the Stanley work[95].

2. Counting the number of times that each diagram can occur in the magnetic system.

A diagrammatic representation of the moments (μ_m) was given by Rushbrook and wood(RW)[96]:-

$$\mu_m = \sum_d \mu_m(d). \tag{4.8.45}$$

However, Stanley and his co-worker Kaplan outlined a diagrammatic representation of the coefficients the spin-spin correlation function(α_l) and ν_l. Here the Hamiltonian is $H = \sum_{ij} J_{ij}\vec{s_i} \cdot \vec{s_j} \equiv \sum_{ij} H_{ij}$, then based on this $\nu_l = \langle S_i \cdot S_j H^l \rangle$ and this is a sum of averages $\langle S_i \cdot S_j \prod H_{ij} \rangle$ of a product of l factors of H_{ij} and one factor of $\vec{S_i} \cdot \vec{S_j}$. Now, for each of the l factors H_{ij} in the product, Stanley and Kaplan (SK) draw a straight line connecting sites i and j; for the factor $\vec{S_i} \cdot \vec{S_j}$, a wavy line connects the given fixed sites i and j. all in all we have $(l+1)$ lines corresponding to the entire product is the diagram $\bar{d}$ associated with that product. Therefore,

$$\nu_l = \sum_{\bar{d}} \nu_l(\bar{d}), \tag{4.8.46}$$

and

$$\alpha_l = \sum_{\bar{d}} \alpha_l(\bar{d}). \tag{4.8.47}$$

Here $\alpha_l(\bar{d}) = \nu_l(\bar{d}) - \sum_{k=0}^{l-1} \sum'_{\bar{d}_a, d_b} \alpha_k(\bar{d}_a)\mu_{l-k}(d_b)$. For this purpose we can use the expansion coefficient as

$$\alpha_l = \bar{S^2}(-2\bar{S^2})^l (J^{m_1}_{ik_1} J^{m_2}_{k_2k_3} ... J^{m_v}_{k_nj})[\alpha_l(\tau)], \tag{4.8.48}$$

here $\sum_{r=1}^{v} m_r = l$, $m_r = 0, 1, ..., l$ and $\bar{S^2} = S(S+1)$. The weight ($[\alpha_l(\tau)]$) for each topological type (τ) is given in the table. Expansions as power series in reciprocal temperature of the zero-field susceptibility of a magnetic system using correlation

Table 4.2: indicates that the relationship between straight lines(l) that can be used for diagrammatic representation, topological type(τ), and the weight ($[\alpha_l(\tau)]$)

$l:\tau$	$[\alpha_l(\tau)]$	$l:\tau$	$[\alpha_l(\tau)]$	$l:\tau$	$[\alpha_l(\tau)]$
0:1	1	5:4	$-\frac{8}{27}$	6:7	$\frac{16}{45}$
1:1	$\frac{1}{3}$	5:5	$\frac{16}{63}$	6:8	$\frac{32}{63}$
2:1	$\frac{2}{9}$	5:6	$-\frac{16}{9}$	6:9	$-\frac{16}{9}$
3:1	$\frac{2}{9}$	5:7	$-\frac{8}{9}$	6:10	$-\frac{32}{9}$
3:2	$-\frac{2}{15}$	5:8	$-\frac{152}{135}$	6:11	$-\frac{16}{9}$
4:1	$\frac{8}{27}$	6:1	$\frac{80}{81}$	6:12	$-\frac{16}{9}$
4:2	$-\frac{8}{45}$	6:2	$-\frac{16}{27}$	6:13	$-\frac{32}{9}$
4:3	$-\frac{8}{15}$	6:3	$-\frac{16}{27}$	6:14	$-\frac{608}{135}$
5:1	$\frac{40}{81}$	6:4	$-\frac{16}{9}$	6:15	$-\frac{304}{135}$
5:2	$-\frac{8}{9}$	6:5	$-\frac{32}{9}$	6:16	$-\frac{16}{15}$
5:3	$-\frac{8}{27}$	6:6	$-\frac{304}{135}$	6:17	$-\frac{160}{65}$

function to order six in β can be defined as:

$$\chi(\beta) = \sum_{m=0}^{n} \sum_{n=0}^{6} d(m,n)\zeta^m t^n, \tag{4.8.49}$$

$$\xi^2(\beta) = \sum_{m=0}^{n} \sum_{n=1}^{6} c(m,n)\zeta^m t^n. \tag{4.8.50}$$

Where $\zeta = \frac{J_2}{J_1}$ and $t = \frac{2S(S+1)J_1}{k_B T}$. The series coefficients d(m,n) and c(m,n) are given:

Spin glass susceptibility (χ_{SG}) is non linear. This is because of the order parameter (q) is non linear i.e. the self-overlap, also called Edwards-Anderson[49] parameter is defined as:

$$q = \frac{1}{N} \sum_i [\langle S_i \rangle^2]_{av}. \tag{4.8.51}$$

This leads to the magnetic Spin glass susceptibility (χ_{SG}) as:

$$\chi_{SG} = \frac{1}{NT^2} \sum_{ij} [\langle S_i S_j \rangle^2]_{av}. \tag{4.8.52}$$

Table 4.3: coefficient of magnetic susceptibility

(m,n)	d(m,n)	(m,n)	d(m,n)	(m,n)	d(m,n)
(0,0)	1	(0,4	$\frac{112}{2025}$	(5,5)	$\frac{2386144}{202625}$
(0,1)	$-\frac{16}{45}$	(1,4)	$-\frac{3728}{2025}$	(0,6)	$\frac{9776}{202625}$
(1,1)	$\frac{16}{15}$	(2,4)	$\frac{5632}{675}$	(1,6)	$-\frac{734176}{637875}$
(0,2)	$\frac{16}{45}$	(3,4)	$-\frac{42256}{2025}$	(2,6)	$\frac{11248}{1215}$
(1,2)	$-\frac{32}{15}$	(4,4)	$\frac{10432}{2025}$	(3,6)	$-\frac{5915984}{91125}$
(2,2)	$\frac{64}{45}$	(0,5)	$-\frac{704}{14175}$	(4,6)	$\frac{5379056}{42525}$
(0,3)	$-\frac{16}{75}$	(1,5)	$\frac{3232}{3375}$	(5,6)	$-\frac{41697584}{212625}$
(1,3)	$\frac{256}{135}$	(2,5)	$-\frac{355376}{30375}$	(6,6)	$\frac{3478912}{1275575}$
(2,3)	$-\frac{928}{135}$	(3,5)	$\frac{202112}{6075}$		
(3,3)	$\frac{1712}{675}$	(4,5)	$-\frac{385984}{6075}$		

Table 4.4: coefficients of correlation function

(m,n)	c(m,n)	(m,n)	c(m,n)	(m,n)	c(m,n)
(0,0)	0	(0,4	$-\frac{18532}{121550625}$	(5,5)	$-\frac{5599272904}{12762815625}$
(0,1)	$-\frac{1}{210}$	(1,4)	$-\frac{5619337}{243101250}$	(0,6)	$-\frac{2088467932}{1340095640625}$
(1,1)	$-\frac{4}{105}$	(2,4)	$-\frac{26529968}{121550625}$	(1,6)	$-\frac{28002872983}{2680191281250}$
(0,2)	$-\frac{44}{3675}$	(3,4)	$-\frac{17916953}{243101250}$	(2,6)	$-\frac{81837440084}{38288446875}$
(1,2)	$-\frac{17}{11025}$	(4,4)	$-\frac{11962192}{121550625}$	(3,6)	$-\frac{337316720399}{536038256250}$
(2,2)	$\frac{368}{11025}$	(0,5)	$-\frac{5243482}{12762815625}$	(4,6)	$-\frac{858172626628}{268019128125}$
(0,3)	$-\frac{2213}{771750}$	(1,5)	$-\frac{45542536}{2552563125}$	(5,6)	$-\frac{2081566923263}{2680191281250}$
(1,3)	$\frac{8576}{165375}$	(2,5)	$-\frac{665249063}{5105126250}$	(6,6)	$-\frac{667883884798}{1340095640625}$
(2,3)	$-\frac{20984}{1157625}$	(3,5)	$-\frac{2177796064}{2552563125}$		
(3,3)	$\frac{60316}{1157625}$	(4,5)	$-\frac{89203154}{364651875}$		

Where the correlation length of the correlation function $[\langle S_i S_j \rangle^2]_{av}$ possibly diverges at $T = T_{SG}$.

We used the Padé approximants (P.A)[97] extensively for the analysis of high-temperature series expansions[98]. A [L, K] Padé approximants to a function $f(x) = \sum_{i=0}^{N} b_i x^i$ is a rational fraction $\frac{P_L(x)}{Q_K(x)}$. Where P_L and Q_K are polynomials with degrees L and K respectively. Therefore,

$$f(x) = \frac{P_L(x)}{Q_K(x)} + O(x^{L+K+1}). \tag{4.8.53}$$

In our case, P.A (L,K) to a series $\chi(\beta) = \sum_{m=0}^{n} \sum_{n=0}^{6} d(m,n) \zeta^m t^n$ or $\xi^2(\beta) = \sum_{m=0}^{n} \sum_{n=1}^{6} c(m,n) \zeta^m t^n$ is a rational fraction i.e.

$$\chi(\beta) or \xi^2(\beta) = \frac{P_L(x)}{Q_K(x)} + O(x^{L+K+1}). \tag{4.8.54}$$

Close to a second-order phase transition at finite temperature T_c^{-1} from a paramagnetic to an ordered state, thermodynamic quantities generally diverge as:

$$\chi(T) \propto (T - T_c)^{-\gamma}, \tag{4.8.55}$$

and

$$\xi^2(T) \propto (T_c - T)^{-2\nu}. \tag{4.8.56}$$

And Padé approximants to the logarithmic derivative $\frac{dln\chi(T)}{dT} \approx \frac{-\gamma}{T - T_c}$ help to determine the critical exponents of susceptibility and correlation function γ and ν respectively.

4.9 Results and Discussion

By using mean-field approximation and experimental values for the Neel temperature and the Curie-Weiss temperature of the materials, we determined the nearest neighbor (nn) and next nearest neighbor (nnn) interaction couplings for the ordered state.

But by taking in to consideration the disordered state i.e. using probability distribution, we have computed both interaction couplings for each concentration. Based on these exchange coupling and using high temperature series expansion extrapolated with Padé approximants we presented concentration dependent transition temperature (Phase diagram) as follows: In this case we can justify that there are spin glass

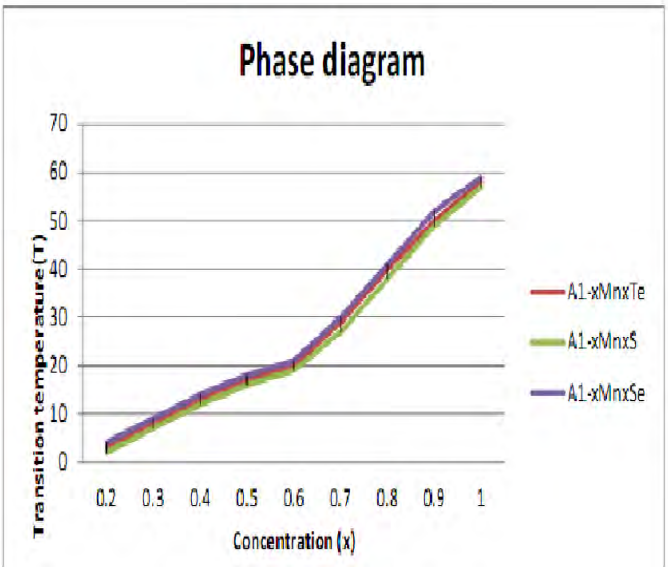

Figure 4.1: *Explains the relationship between the magnetic phase transition temperatures verses magnetic impurity concentration of* $A_{(1-x)}Mn_xA'$.

phase in range $(0.2 \leq x < 0.6)$ and antiferromagnetism in range $(0.6 < x \leq 1)$ based on exchange interaction couplings calculations.

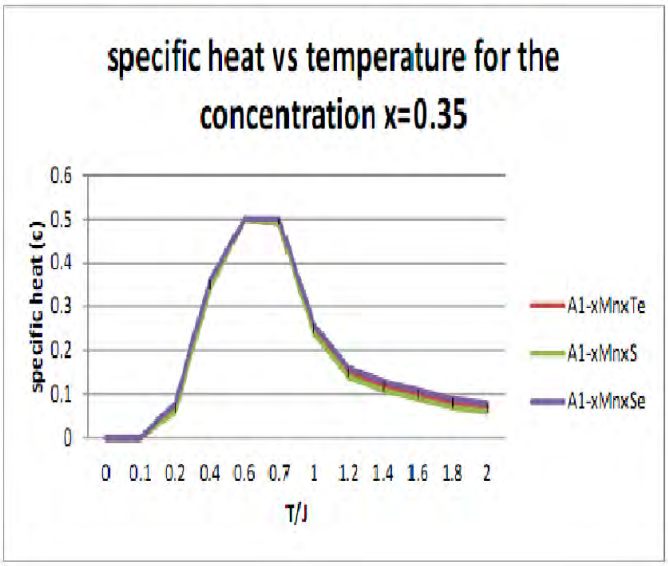

Figure 4.2: *Schematic representation of magnetic specific heat vs. temperature for the materials* $A_{(1-x)}Mn_xA'$.

4.10 Conclusions

In this part of the dissertation exchange integrals (J_1 and J_2) for nearest neighbor (nn) and next nearest neighbor interactions (nnn) using mean-field approximation in concentration range ($0.6 \leq x \leq 1$) and taking in to consideration the dilution problem we used probability distribution in range ($0.2 \leq x < 0.6$) for the systems were computed. We used these values for magnetic susceptibility and magnetic specific heat calculations. In order to determine the susceptibility and specific heat, we implemented high temperature series expansion and *Padé* approximants at the critical region. Different magnetic phases such as (spin glass, antiferromagnetic and paramagnetic) based on their concentration ranges were established and the findings are in agreement with previous studies. The critical exponents associated with magnetic

susceptibility and correlation function $\gamma = 1.38 \pm 0.1$ and $\nu = 0.8 \pm 0.1$ respectively were also obtained.

Chapter 5

Summery and Future plan

This dissertation reports the results of Monte Carlo simulation of finite dimensional spin glass systems with distance dependent interaction and theoretical study of spin glass state in diluted magnetic semiconductors. In the first part of the study we have studied two dimensional Ising spin glass model. In this case since the system is a disordered system, we have free energy land escapes. To overcome the energy land escapes and to minimize the relaxation time of the simulation we employed the parallel tempering Monte Carlo simulation. The model studied does not provide any evidence for phase transition for nearest neighbor interactions. This is consistent with the present spin glass theory. In order to show the spin glass phase transition we considered the long-range interaction model i.e. diluted version of power law decaying interaction coupling. Int he model every spin is connected with a finite number of other spins and we have chosen an average coordination number z=6. The results we obtained are summarized as follows:

1.The parallel tempering Monte Carlo simulation reduces the relaxation time and speed up the equilibration of the simulation and all data that we have shown are

thermalized.

2. We have simulated different systems with different geometrical organization of random interactions. For each system we have simulated two replicas in order to study the overlap order parameter.

3. We have computed the overlap distribution function for $\rho = 2; 3; 4$. In the first two cases we found evidence for the existence of a phase transition from the paramagnetic to the spin glass phase. In the last case, double peaked distributions, typical of the spin glass phase are displayed at low T for small sizes. However, the T_c at which the conversion from single peak to double peak occurs, appear to continuously decrease with L. This is in agreement with the fact that the value $\rho = 4.0$ indicates the cross over at which long-range systems whose interaction decrease with $r^{-\rho}$ become effectively short range. Since in 2D the short-range spin glass phase does not exist, T_c must go to zero in the proximity of $\rho = 4$.

In the second part of our study we considered the vector spin to examine the stability of the spin glass phase in the 3D Heisenberg model. We know that some physical quantities diverge seemingly to infinity at the critical point. This raises a challenge for numerical simulations to see the critical phenomena since we have to simulate systems at different sizes and in order to avoid this problem we used the finite size scaling for the numerical simulation. Here, we used classical Heisenberg spin glass in 3D with the interaction following the Edwards-Anderson model and by calculating Binder parameter we found the absence of finite temperature spin glass phase transition. When we examined non linear susceptibility it also appears that there was clear indication of the absence of finite temperature phase transition.

In the third part of our study we considered theoretical analysis (high temperature series expansion extrapolated with Padé approximants) to identify the magnetic properties at the critical region. In this case, the exchange integrals ($J_1 and J_2$) for nearest neighbor (nn) and next nearest neighbor interactions (nnn) using mean-field approximation in concentration range ($0.6 \leq x \leq 1$) and taking in to consideration the dilution problem we used probability distribution in range ($0.2 \leq x < 0.6$) for the systems were computed. We used these values for magnetic susceptibility and magnetic specific heat calculations. In order to determine the susceptibility and specific heat, we used high temperature series expansion and Padé approximants at the critical region. Different magnetic phases such as (spin glass, antiferromagnetic and paramagnetic) based on their concentration ranges were established and the findings are in agreement with previous studies. The critical exponents associated with magnetic susceptibility and correlation function $\gamma = 1.38 \pm 0.1$ and $\nu = 0.8 \pm o.1$ respectively were also obtained.

For future we are planning to extend this work to spin glass superconductor which is a very exciting research area in recent time. We also intend to study chiral glass using Heisenberg spin model in 3D.

Appendix

2 Appendix A: Figures for different system sizes and ρ values

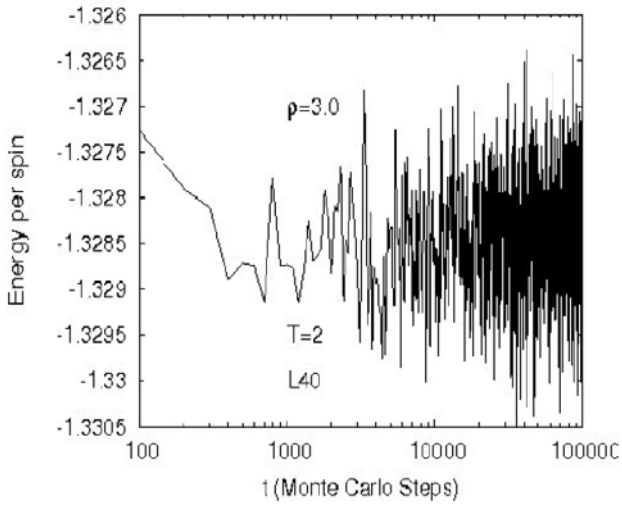

Figure A.2: Schematic representation of Energy per spin versus t(Monte Carlo steps) for $L = 40$, $T = 2$, $\rho = 3.0$.

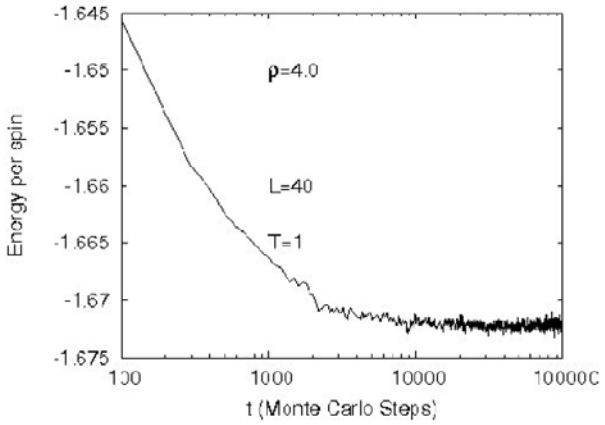

Figure A.2: Schematic representation of Energy per spin versus t(Monte Carlo steps) for$L = 40$, $T = 1$, and $\rho = 4.0$.

3 Appendix B: Binder parameter

Lets assume that the spin glass order parameter as $q = (q_1, q_2, q_3, ..., q_n)$. However each order parameter (q_i) is independent and has either bimodal or Gaussian type of probability distribution:-

$$p(q_i) = \frac{1}{\sigma\sqrt{2\pi}} exp(\frac{q_i^2}{2\sigma^2}). \tag{3.1}$$

Now lets consider a quantity which is rotationally invariant and in order to represent the fact that the spins rotate collectively. By definition:-

$$Q^2 = q_1^2 + q_2^2 + ... + q_n^2. \tag{3.2}$$

This leads to

$$\langle Q^2 \rangle = \langle q_1^2 \rangle + \langle q_2^2 \rangle + ... + \langle q_n^2 \rangle = n\lambda^2. \tag{3.3}$$

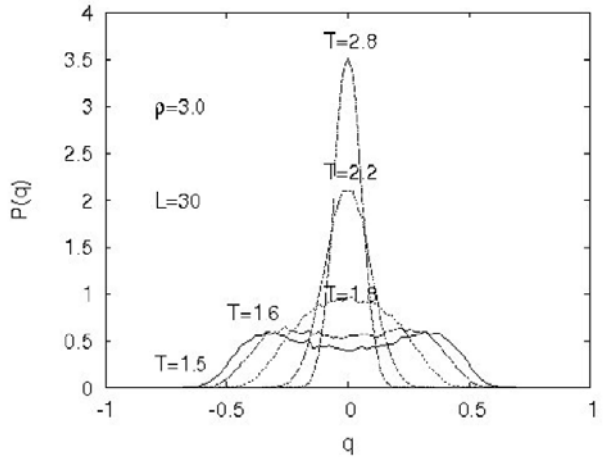

Figure A.2: Schematic representation of p(q) versus q for $L = 30$, $\rho = 3.0$, and $T = 1.5, 1.6, 1.8, 2.2, 2.8$.

and

$$Q^4 = q_1^4 + q_2^4 + ... + q_n^4 + \sum_{ij} q_i^2 q_j^2. \tag{3.4}$$

But if we take thermal average of this eq.(3.4), we get:-

$$\langle Q^4 \rangle = n\langle q_1^4 \rangle + n(n-1)\langle q_i^2 \rangle^2 = 3n\lambda^4 + n(n-1)\lambda^4. \tag{3.5}$$

This implies that:-

$$\langle Q^4 \rangle = (n^2 + 2n)\lambda^4. \tag{3.6}$$

Therefore if we take the ratio of the fourth and and the second moments:

$$\frac{\langle Q^4 \rangle}{\langle Q^2 \rangle^2} = \frac{n+2}{n}. \tag{3.7}$$

For Heisenberg spin model n=9 and Binder parameter would be:-

$$g_L = \frac{1}{2}[11 - 9\frac{\langle Q^4 \rangle}{\langle Q^2 \rangle^2}] \tag{3.8}$$

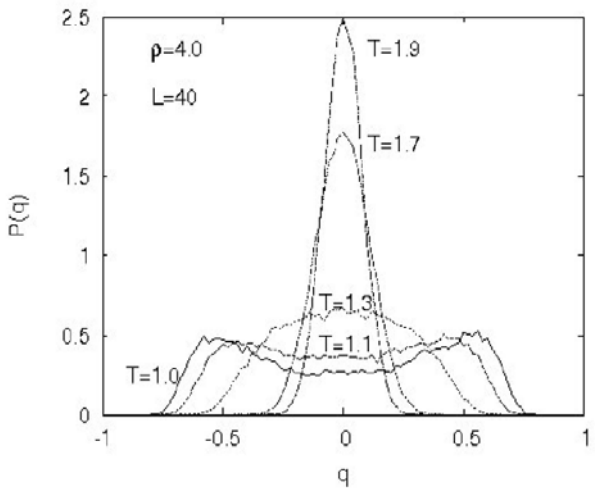

Figure A.2: Schematic representation of p(q) versus q for $L = 10, 20, 30, 40$ $\rho = 4.0$, $T = 1.0, 1.1, 1.3, 1.7, 1.9$.

4 Appendix C: derivation for diagrammatical representation

As we defined in section(4.3) above:

$$\nu_l = \langle S_i \cdot S_j H^l \rangle = \frac{Tr\{S_i \cdot S_j H^l e^{-\beta H}\}}{Tr\{e^{-\beta H}\}} \tag{4.1}$$

and

$$\mu_m = \langle H^m \rangle = \frac{Tr\{H^m e^{-\beta.H}\}}{Tr\{e^{-\beta H}\}} \tag{4.2}$$

Now lets assume that the hamiltonian for the spin-spin exchange interaction:

$$H = \sum_{\langle ij \rangle} J_{ij} \vec{s_i} \cdot \vec{s_j}, \tag{4.3}$$

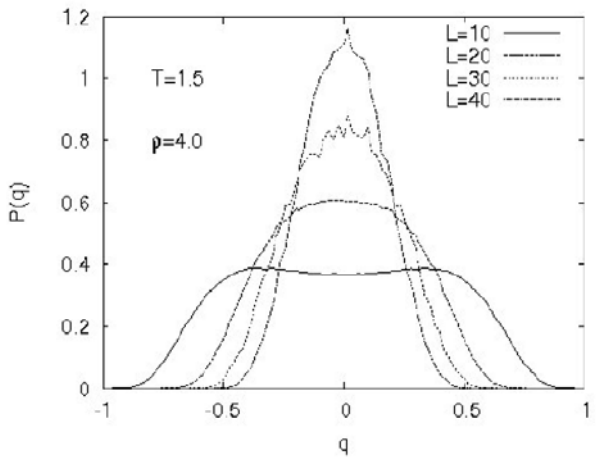

Figure A.2: Schematic representation of p(q) versus q for $L = 10, 20, 30, 40$, $\rho = 4.0$, $T = 1.5$.

where $\langle ij \rangle$ refers that summation over all different pairs of nearest neighbors. To obtain expansion coefficient for the spin-spin correlation function (α_l) first we have to evaluate (μ_m) and (ν_l). Then from eqs.(4.2) and (4.3)

$$\mu_m = (-J_{ij})^m \frac{Tr\{(\sum_{\langle ij \rangle} \vec{s_i} \cdot \vec{s_j})^m e^{-\beta H}\}}{Tr\{e^{-\beta H}\}}, \tag{4.4}$$

with m pairs in the trace, is associated with a diagram containing m lines. Representing such diagrams by d, we get

$$\mu_m = (-J_{ij})^m \sum_d \mu_m(d). \tag{4.5}$$

Here

$$\mu_m(d) = \sum_c \frac{Tr\{(\vec{s_i} \cdot \vec{s_j})...(\vec{s_k} \cdot \vec{s_t}) e^{-\beta H}\}}{Tr\{e^{-\beta H}\}}, \tag{4.6}$$

and c indicates that the combination of pairs of spins at two sites that corresponds to the given diagram. In the same way one can represent

$$\nu_l = (-J_{ij})^l \sum_{\bar{d}} \nu_l(\bar{d}). \tag{4.7}$$

since in this case in addition to straight lines for each pairs of spins there is one wavy line,the diagram is denoted by $\bar{d}$

Bibliography

[1] Kar P., Nadler W., and Hansmann U. H. E. Microcanonical replica exchange molecular dynamics simulation of proteins. Phys. Rev. E **80** :5(2009)056703.

[2] Nieto, Roma F., Risau-Gusman S., Ramirez-pastor, A.,Nieto F., and vogel E. The ground state energy of the edwards-anderson spin glasses model with parallel tempering Monte Carlo algorithm. Physica A: statistical mechanics and its applications **388**:14(2009)2821.

[3] H. T. Diep. Frustrated Spin Systems (World Scientific, Singapore, 2005).

[4] K. Binder and A. P. Young. Spin glasses: Experimental facts, theoretical concepts and open questions. Rev. Mod. Phys. **58**,(1986)801.

[5] M. Mezard, G. Parisi, and M. A. Virasoro. Spin Glass Theory and Beyond (World Scientific, Singapore, 1987).

[6] A. P. Young, ed. Spin Glasses and Random Fields (World Scientific, Singapore, 1998).

[7] Gordon Moore.Cramming more components onto integrated circuits. Electronics,**38**,(1965).

[8] H. Ohno. Properties of ferromagnetic III-V semiconductors. Journal of Magnetism and Magnetic Materials, **200** (1999)110.

[9] J. K. Furdyna. Diluted magnetic semiconductors. J. Appl. Phy. **64**,(1988)R29.

[10] D. Ferrand, J. Cibert, A. Wasiela, C. Bourgognon, S. Tatarenko, G. Fishman, T. T. Andearczyk, J. Jaroszynski, S. Kolesnik, T. Dietl, B. Barbara, and D. Dufeu.Carrier-induced ferromagnetism in $p - Zn_{1-x}Mn_xTe$. Phys. Rev. B **63**,(2001) 085201.

[11] G. Bastard, C. Rigaux, Y. Guldner, A. Mycielski, J. K. Furdyna, and D. P. Mullin. Interband Magnetoabsorption in Semimagnetic Semiconductor Alloys $Hg_{1-x}Mn_xTe$ with a Positive Energy Gap. Phys. Rev. B, **24**(1961,1981).

[12] R. R. Galazka, S. Nagata,and P. H. Keesom. Paramagnetic-spin-glass- antiferromagnetic phase-transitions in $Cd_{1-x}Mn_xTe$ from specific-heat and magnetic-susceptibility measurements. Phys. Rev. B, **22**,(1980)3344.

[13] R. R. Galazka. Physics of Semiconductors. Inst. Phys. Conf. ser., **43**,(1979)133.

[14] H. Ohno, D. Chiba, F. Matsukara, T. Omiya, E. Abe, T. Dietl, Y. Ohno, and K. Ohtani. Electric-field control of ferromagnetism. Nature, **408**, (2000)944.

[15] H. Munekata, H. Ohno, S. Von Molnar, Armin Segmaller, L. L. Chang, and L. Esaki. Diluted magnetic III-V semiconductors. Phys. Rev. Lett.**63**, (1989)1849.

[16] H. Ohno, H. Munekata, T. Penney, S. Von Molnar, and L. L. Chang. Magneto transport properties of p-type (In,Mn)As diluted magnetic III-V semiconductors. Phys. Rev. Lett.**68**,(1992)2664.

[17] C. Kittel,In F. Seitz, D. Turnbull, and H. Ehrenreich, editors. Solid State Physics **22**,1(Academic Press, New York, 1968).

[18] H. Ohno, A. Shen, F. Matsukura, A. Oiwa, A. Endo, S. Katsu Moto, and Y. Iye. Magneto-resistance effect and interlayer coupling of (Ga,Mn)As. Appl. Phys. Lett.**69**, (1996)363.

[19] T. Jungwirth, J. Sinova, J. Masek, J. Kucera, and A. H. Macdonald. Theory of ferromagnetic (III,Mn)V semiconductors. Rev. Mod. Phys. **78**,(2006)809.

[20] K. Y. Wang, K. W. Edmonds, R. P. Campion, L. X. Zhao, A. C. Neumann, C. T. Foxon, B. L. Gallagher, and P. C. Main (2002) in proceedings of the ICPS-26(IOP,UK)58.

[21] K. W. Edmonds, K. Y. Wang, R. P. Campion, A. C. Neumann, N. R. S. Farley, B. L. Gallagher, C. T. Foxon. High-Curie-temperature $Ga_{1-x}Mn_xAs$ obtained by resistance-monitored annealing. Appl. Phys. Lett.**81**,(2002)4991.

[22] D. Chiba, K. Takamura, F. Matsukara, and H. Ohno. Effect of low temperature annealing on (Ga,Mn)As trilayer Structures. Appl. Phys. Lett. **82**,(2003)3020.

[23] M. A. Ruderman and C. Kittel. Indirect Exchange Coupling of Nuclear Magnetic Moments by Conduction Electrons. Phys. Rev.,**96**,(1954)99.

[24] T. Kasuya. A Theory of Metallic Ferro- and Antiferromagnetism on Zener's Model. Phys. Rev., **106**,(1957)893.

[25] K. Yosida. Magnetic properties of Cu-Mn alloys. Prog. Theor. Phys.,**16**,(1956)45.

[26] C. Zener. Interaction between the d shells in the transition metals. Phys. Rev.,**81**,(1950)440.

[27] David D. Awschalom, Michael E. Flatte, and Nitin samarth. Spintronics(scientific American, June,2002).

[28] Igor Zutic,Jaroslov Fabian, and S. Das Sarma. Spintronics fundamentals and applications. Rev. Mod. Phys.,**76**,(2004)323.

[29] S. Datta and B. Das. Electronic analog of the electro-optic modulator. Appl. Phys. Lett.,**56**,(1990)665.

[30] M. Johnson. Spin injection in metals and semiconductors. Sci.Technol, **17**,(2002)298.

[31] Brush S. G. History of the Lenz-Ising model. Rev. Mod. Phys.**39**:4(1967),883

[32] Ferdinand, Arthur, Fisher, and E. Michael. Bounded and inhomogeneous ising Models specific-Heat Anomaly of a finite lattice. Phys.Rev.,**185**:2, (1969)832. DOI:10.1103/Phys. Rev.185.832.

[33] Newman M. E. J., and Barkema G. T. Monte Carlo methods in statistical physics(Oxford University press,1999).

[34] D. Frenkel and B. Smit. Understanding molecular simulation from algorithms to application(Academic press,1996).

[35] M. H. Kalos and P. A. Whitlock. Monte Carlo methods (Wiley, New York, 1986).

[36] W. H. Press, B. P. Flannery, S. A. Teukolsky, and W. T. Vetterling. Numerical Recipes: The art of scientific computing (Cambridge University press, Cambridge, 1986).

[37] N. G.van Kampen. Stochastic process in physics and chemistry(North-Holland, Amsterdam,1981).

[38] Metropolis, N. Rosenbluth, M. Teller, A., and Teller E. Equation of state calculations by fast computing machines. J. Chem. Phys.**21** (1953)1087.

[39] Falcoioni M., Deem M. W.. A biased Monte Carlo scheme for zeolite structure solution. J. Chem. Phys., **110**,(1999)1754.

[40] Wu M. G., Deem M. W. Efficient Monte Carlo methods for cyclic peptides. Mol. Phys. **97**,(1999)559.

[41] Yan Q. L., Pablo J. J. de. Hyper parallel tempering Monte Carlo: Application to the Lennard-Jones fluid and the restricted primitive model. J. Chem. Phys.**111**,(1999)9509.

[42] C. J. Geyer and E. A. Thompson. Annealing marcov chain Monte Carlo with applications to the ancestral inference. J. Am. Stat. soc.,**90**,(1995)909.

[43] S. Krickpatrick, C. D. Gelatt Jr., and M. P. Vecchi. Optimization by simulated annealing. Science,**220**,(1983)671.

[44] Amit, D. J. Modeling brain function(Cambridge University press,1989).

[45] K. Hukushima and K. Nemato. Exchange Monte Carlo method and application to spin glass simulations. J. Phys. Soc. Jpn. **65**, 1604(1996).

[46] Katzgraber H. G., Trebst S., Huse D. A., and Troyer M. Feedback-optimized parallel tempering monte carlo. J. Stat. Mech. P03018 (2006).

[47] Bittner E., Nußbaumer A., and Janke W. Make life simple: Unleash the full power of the parallel tempering algorithm. Phys. Rev. Lett. **101** ,(2008)130603.

[48] V. Canella and J. A. Mydosh. Magnetic Ordering in Gold-Iron alloys. Phys. Rev. B. **6**,(1972)4220.

[49] Edwards, S. F. Anderson, P. W. Theory of spin glasses. J. Phys. metal Phys. **5**, (1975)965.

[50] J. W. Landry and S. N. Coppersmith. Ground states of two-dimensional Edwards-Anderson spin glasses. Phys. Rev. B, **65**,(2002)134404

[51] Stefan Boettcher. Stiffness of the Edwards-Anderson model in all dimensions. PRL. **95**,(2005)197205

[52] R. Serral Gracia and Th. M. Nieuwenhuizen. Quantum spherical spin models. Phys. Rev. **E** 69056119 (2004) [cond-mat/0304150].

[53] L. Leuzzi, G. Parisi, F. Ricci-Tersenghi, J. J. Ruiz-Lorenzo. Bond Diluted Levy spin-glass model and a new finite-size scaling method to determine a phase transition. Philosophical Magazine 2010, 1-9, iFirst.

[54] W. Nolting. Grundkurs Theoretishe physik6 - statistische physik5(Auflage, springer verlag, 2005).

[55] J. J. Binney, N. J. Dowrick, A. J. Fisher, and M. E. J. Newman. The theory of critical phenomena- An introduction to renormalization group(Oxford science publication, 1992).

[56] Helmut G. Katzgraber and L. W. Lee. Correlation length of the two-dimentional Ising spin glass with bimodal interactions. Phys. Rev. B **71**,(2002)134404

[57] A. J. Bray and M. A. Moore. Is mean-field theory valid for spin glasses? J. phys. C: solid state phys. **15**(1982),3897, DOI:10.1088/0022-3719/15/18/007.

[58] A. J. Bray and M. A. Moore. Chaotic nature of the spin-glass phase. Phys. Rev. Lett.,**58**(1987)57

[59] Swendsen R. H., and Wang J. S. Non universal critical dynamics in Monte Carlo simulations. Phys. Rev. Lett. **58**:2(1987)86.

[60] C. Itzykson, J. M. Droufe. Statistical Field Theory (Cambridge University Press, 1989).

[61] L. Leuzzi, G.parisi, F.Ricci-Tersenghi, and J. J. Ruiz-Lorenzo. Diluted one-dimentional spin glasses with power law decaying interactions. PRL **101**,(2008)107203 .

[62] R. N. Bhatt and A. P. Young. Long range Ising spin glasses: Critical behavior and utrametricity. Journal of magnetism and magnetic materials **54**(1986).

[63] R. H. Swendsen and J. Wang. Replica Monte Carlo simulation of spin-glasses. Phys.Rev. Lett. **57**,(1986)2607

[64] E. Marinari and G. Parisi. Simulated tempering: A new Monte Carlo scheme. Europhys. Lett. **19**,(1992)451

[65] A .P. Lyubartsev, A.A. Martsinovski, S. V. Shevkunov, and P. N. Vorontsov-Velyaminov. New approach to Monte Carlo calculation of the free energy: Method of expanded ensembles. J.Chem.Phys.**86**,(1992)1776

[66] J.Cardy. Scaling and renormalization in statistical Physics(Cambridge University Press,1996).

[67] J. A. Olive, A. P. Young, and D. Sherrington. Computer simulation of the three-dimensional short-range Heisenberg spin glass. Phys. Rev.B **34**,(1986)6341.

[68] F. Matsubara, T. Iyota, and S. Inawashiro. Phase diagram of a short-Range $\pm J$ Heisenberg Modelin three dimensions. J. Phys. Soc.Jpn. **60**,(1991)4022.

[69] H. Kawamura. Chiral ordering in Heisenberg spin glasses in two and three dimensions. Phys. Rev. Lett.**68**,(1992)3785.

[70] H. Kawamura. Dynamical simulation of spin-glass and chiral-glass orderings in three-dimensional Heisenberg spin glasses. Phys. Rev. Lett. **80**,(1998)5421.

[71] H. Kawamura. Chiral scenario of the spin glass ordering. arXiv: 0907.4218V2 [cond-mat.dis-nn](2010)

[72] R. N. Bhatt and P. Young. Search for a transition in the three-dimensional Ising $\pm J$ Spin-Glass. Phys. Rev. B. **54**,(1985)924.

[73] K. Binder. Finite size scaling analysis of Ising model block distribution functions. Z. Phys. B. **43**,(1981)119.

[74] H. -O. Heuer. A fast vectorized Fortran 77 program for the Monte Carlo simulation of the three-dimensional Ising system. Comp. Phys. Comm. **59**,(1990)387.

[75] H. Rieger. Fast vectorized algorithm for the three dimensional random field Ising model. J. Stat. Phys. **70**,(1993)1063.

[76] N. Kawashima, N. Ito and Y. Kanada. Algorithms for Monte Carlo simulations of the Ising models on a simple cubic lattice. Int. J. Mod. Phys. **C4**,(1993)525.

[77] K. Fabricius, A. Klumper, U. Low, B. Buchner, T. Lorenz, G. Dhalenne, and A. Revcolevschi. Re-examination of the microscopic couplings of the quasi-one-dimensional antiferromagnet $CuGeO_3$. Phys. Rev. B,**57**,(1998)1102.

[78] H. G. Evertz. The loop algorithm. Adv. Phys. ,**52**,(2003)1.

[79] R. J. Bursill, T. Xiang,and G. A. Gehring. The density matrix renormalization group for a quantum spin chain at non-zero temperature. J. Phys.: Condens. Matter, **66**,(1997)2221.

[80] X. Q. Wang and T. Xiang. Transfer-matrix density-matrix renormalization-group theory for thermodynamics of one-dimensional quantum systems. Phys. Rev. B, **56**,(1998)5061.

[81] G. S.Rushbrooke, G. A. Baker, Jr. ,and P. J. Wood. Heisenberg model. In C. Domb and J. Lebowitz, editors. Phase transition and critical phenomena ,volume 3,chapter 5, pages 245-356(AcademicPress, NewYork,1974).

[82] R. Navarro. Application of high-and low-temperature series expansions to two dimensional magnetic systems. L. J. deJongh, editor. Magnetic properities of layered

transition metal compounds ,volume 9, chapter 6, pages105-190(Kluwer Academic Publishers, Dordrecht, Netherlands,1990).

[83] C. Domb and M. S. Green. Phase transitions and critical phenomena, volume 3(Academic Press, 1974).

[84] M. P. Gelfand, R. R. P. Singh, and D. A. Huse. Perturbative expansions for quantum many-body systems. J. Stat. Phys., **59**,(1990)1093.

[85] J. K. Furdyna. Diluted magnetic semiconductors. J. Appl. Phys. **64**,(1988)R29.

[86] Shin-ichi Endoh, Fumitaka Matsubara and Takayuki Shirakura. Stiffness of the Heisenberg spin-glass model at zero and finite temperatures in three dimensions. arXiv: cond-mat/0104021v1 [cond-mat.dis-nn] (2001).

[87] J. Ricardo de souse and N. S. Branco. Two-dimensional quantum spin-1/2 Heisenberg model with competing interactions. Physical Review B **72**,(2005)134421.

[88] Hikaru Kawamura. The ordering of XY spin glass. arXiv: 1102.3496V1 [con-mat.dis-nn](2011).

[89] R. Masrour, M. Hamedoun and A. Benyoussef. Magnetic properties of semi-magnetic semiconductor materials. International Journal of the physical sciences **6**:16(2011)4020.

[90] Holland W. E, Brown H. A . Application of the Weiss molecular field theory to the B-site spinel. Phys-Stat. Sol.(A), **10**(1972)249.

[91] Moron M. C . The critical temperature and exchange interactions of an S = 5/2 Heisenberg antiferromagnet on an f.c.c. lattice. J. Phys.Condensed Matter., **8**(1996)11141.

[92] R. Masrour, M. Hamedoun, and A. Benyoussef. Study of the magnetic property in the systems $K_2Cu_xMn_{1-x}F_4$. Chinese Journal of Physics **47**:1,(2009)71

[93] N. W. Ashcroft, N. D. Marmin. Solid state physics (Harcourt college publishers, USA, 1976).

[94] Tawardowski A, Swagten H.J.M, de Jonge WJM, Demianiuk M . Magnetic behavior of the diluted magnetic semiconductor Zn1-xMnxSe. Phys Rev. B., **36**,(1987)713.

[95] Stanley H. E, Kaplan T. A . High-temperature expansions-the classical Heisenberg model. Phys. Rev. Lett., **16**,(1966)981.

[96] G. S. Rushbrooke and P. J. Wood. On the Curie points and high temperature susceptibilities of Heisenberg model ferromagnetics. International Journal at the Interface Between Chemistry and Physics, **1**:3, (1958)257.

[97] G. A. Baker, P. Graves Moris (Eds.). Pad Approximants(Addison-Wesley, London, 1981).

[98] M. Roger. Differential approximants: An accurate interpolation for high-temperature series expansions to low-temperature behavior in two-dimensional ferromagnets. Phys. Rev. B **58**:17,(1998)11115.

PUBLICATIONS

1.Habte Dulla Berry and Pooran Singh,"Monte Carlo simulation of 2D Ising spin glass system with power law interaction couplings", Journal of superconductivity and novel magnetism,**26**:4, 991-994 (2013) DOI 10.1007/s10948-012-1908-3.

2. Habte Dulla Berry and Pooran Singh, "The Role of Parallel Tempering Monte Carlo Simulation in 2D Ising Spin Glass System with Distance Dependent Interaction", Journal of physical sciences and application **2**:7,216-223(2012).

3.Habte Dulla Berry and Pooran Singh,"Monte Carlo Simulation of Spin Glasses Using Vector Spin Model in 3D",Journal of physical sciences and application **2**:9,340-344(2012) .

4.Habte Dulla Berry and Pooran Singh, "The study of magnetic properties of $A_{1-x}Mn_xA'$ (A=Zn,Cd and A'=S,Te,Se) at critical region using high temperature expansion extrapolated with *Padé* approximants" has been accepted for publication and under press, Journal of physical review and research international.

PAPER PRESENTATION IN INTERNATIONAL AND NATIONAL CONFERENCES

1.Habte Dulla Berry and Pooran Singh, Monte Carlo simulation of 2D Ising spin glass system with power law interaction couplings, the 3^{rd} international conference in superconductivity and magnetism(ICSM2012) ,Istanbul, Turkey. April 29-May 4, 2012.

2.Habte Dulla Berry and Pooran Singh, Monte Carlo Simulation of Spin Glasses Using Vector Spin Model in 3D,The 7th national conference of the Ethiopian physical society, Mekelle University. Fab. 02-03,2013

DECLARATION

I hereby declare that this PhD dissertation is my original work and has not been presented for a degree in any other University and that all source of materials used for the dissertation have been duly acknowledged.

Name: Habte Dulla

Signature: _____

email: habtix07@gmail.com

This PhD dissertation has been submitted for examination with my approval as University advisor.

Name: Prof. P. Singh

Signature: _____

Place and date of submission:

Department of Physics

Addis Ababa University

March, 2013